NASA Contractor Report 195004

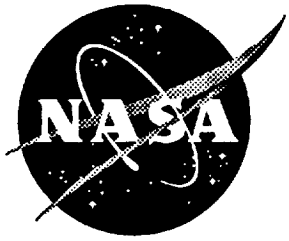

# Multi-Lab Comparison of R-Curve Methodologies: Alloy 2024-T3

Anthony P. Reynolds
*Analytical Services & Materials, Inc., Hampton, Virginia*



Contract NAS1-19708
October 1994

National Aeronautics and
Space Administration
Langley Research Center
Hampton, Virginia 23681-0001

# MULTI-LAB COMPARISON OF R-CURVE METHODOLOGIES: ALLOY 2024-T3

Anthony P. Reynolds
Analytical Services & Materials, Inc.
107 Research Drive
Hampton, VA 23666

## ABSTRACT

In an effort to determine an optimum method for ranking the fracture toughness of developmental aluminum alloys over a wide range of fracture toughness/strength combinations, five labs performed K and/or J based fracture tests on aluminum alloy 2024-T3. Two material thicknesses were examined: 0.063 in. and 0.125 in. Middle crack tension and compact tension specimens were excised from 60 in. wide middle crack tension panels which had been previously tested at Boeing. The crack resistance curves generated were compared to the R-curves from 60 in. wide specimens. The experimental program indicated that effective stress intensity from secant compliance based crack length and stress intensity calculated from J-integral testing were equivalent. In addition, comparison of different specimen sizes and configurations indicated that standard validity requirements for compact tension specimens may be overly restrictive.

## NOMENCLATURE

$a_0$ initial crack length, in.

$a_{eff}$ effective crack length, in.

$a_{phys}$ physical crack length, in.

B specimen thickness, in.

$b_0$ initial uncracked ligament, in.

$b_f$ final uncracked ligament, in.

E Young's modulus, Msi.

$J_{IC}$ critical J-integral value for crack initiation, $lbf/in^2$.

$K_{app}$ apparent stress intensity at failure. Calculated at the maximum load in an R-curve test using the initial crack length, $ksi\sqrt{in}$.

$K_c$ critical stress intensity, calculated at the maximum load in an r-curve test, using the effective crack length, ksi$\sqrt{in}$.

$K_{eff}$ effective stress intensity calculated using $a_{eff}$, ksi$\sqrt{in}$.

$K_{IC}$ critical, plane strain, stress intensity value for crack initiation, ksi$\sqrt{in}$.

$K_J$ stress intensity calculated from applied J, ksi$\sqrt{in}$.

P load, lbf.

W specimen width, in.

$\delta$ load-line displacement, in.

$\sigma_{net}$ net-section stress, ksi.

$\sigma_{ys}$ yield strength, ksi.

## INTRODUCTION

For the last 4 years a significant effort in aluminum alloy development for application on subsonic and supersonic commercial transport aircraft has been supported by NASA. Key property goals for alloy development include substantial improvements over present state of the art alloys in strength, and fracture toughness as measured by $K_C$ (critical stress intensity) or $K_{app}$ (apparent stress intensity at failure.) $K_C$ and $K_{app}$ are measures of plane stress fracture toughness appropriate for material in sheet product form. Retention of the improved properties after long term exposure at elevated temperatures is an important consideration for application on supersonic transport aircraft.

Candidate aluminum alloys have been produced by several materials manufacturers. These same alloys have been characterized by the materials manufacturers, airframe manufacturers and by researchers at NASA Langley Research Center and the University of Virginia, but not all of the alloys have been characterized by all of the labs. For many properties of interest, e.g. yield and ultimate tensile strengths, this does not lead to any ambiguity when the candidate alloys are compared. When fracture toughness is the property of interest, lab to lab variations in test methods lead to difficulty in making comparisons between alloys.

Airframe manufacturers, who will ultimately be responsible for incorporating new alloys into aerostructures, have traditionally used $K_C$ or $K_{app}$ as fracture toughness design parameters. There are no standard methods for measurement of these parameters; but valid $K_C$ and $K_{app}$ numbers can in general only be obtained by testing of wide, center cracked panels (middle crack tension specimens). For medium

strength, high toughness materials like 2024-T3, panel widths of 60 inches or greater may be required.

For the purposes of the NASA sponsored alloy development program, fracture toughness test and analysis method which accurately rank the toughness of the candidate alloys on a relative basis are required. The airframe manufacturers would like to have the relative ranking of the alloys based on wide panel test data. This type of data would provide what the airframe manufacturers perceive as an absolute ranking of the developmental alloys versus the alloys with which they are already familiar. Unfortunately, wide panel testing of developmental alloys is not practical for several reasons. First, the candidate alloys are not all being produced in full size ingots: in some cases, maximum sheet width is less than 24 in. and total material quantities are limited. Second, because thermal stability is a requirement for some of the candidate alloys, testing of wide panel specimens would require the use of large ovens for potentially very long times in order to perform fracture tests on exposed material. Third, the capability for performing wide panel tests is not available at all of the labs participating in the alloy development program.

The airframe manufacturers desired method for ranking fracture toughness, and the limitations imposed by an alloys development program are at odds. The objective of the 2024-T3 fracture toughness round robin program is to circumvent the limits imposed by the nature of the alloy development program by providing a small specimen fracture toughness test method which can be accurately related to material performance in a wide panel fracture test. This goal can be attained only by the parallel development of an appropriate test technique and an analytical method which will relate the test results to wide panel data. The remainder of this report is devoted to a review of the experimental portion of the round robin program.

## EXPERIMENTAL

Five labs participated in the experimental portion of the round robin program: ALCOA, Boeing, Fracture Technology Associates (FA), NASA LaRC, and the University of Virginia (UVA). The Boeing tests were contracted to Fatigue Technology Incorporated (FTI). Material for testing was provided by Boeing. Alloy 2024-T3 sheet in 0.063 in. and 0.125 in. gages was distributed to all of the participating labs. The material was cut from 60 in. wide middle crack tension panels which had previously been tested at Boeing. The decision to use this material was based on two factors: 1)availability and, 2) a direct comparison between small coupon results and wide panel results from identical material could be made. Specimen types were either middle crack tension, MT, or compact tension, CT, with size left up to individual labs. The test specimen configurations are illustrated in figure 1. All tests were to be performed in accordance with ASTM standards E-561 or E-1152. Information regarding J and K solutions for compact and middle crack tension specimens maybe found in the referenced ASTM standards. If tests were performed in accordance with E-561, physical crack length measurements were required so that the data could be subjected to a J integral analysis. Some labs did not comply with the requirement for

physical crack length measurement. All of the data were analyzed using the K-R methodology with secant compliance crack length ($a_{eff}$). The data sets which included sufficient physical crack length measurements were also analyzed using the J-integral method.

The experimental programs undertaken at each lab are detailed in table 1. In the table, specimen size refers to the width of MT and CT specimens, gages refers to material thicknesses tested, and Δa is the crack extension measurement method.

**TABLE 1. Details of Laboratory Experimental Efforts**

| Lab | Specimen Type/Size | Gages | $a_{phys}$ measured? | Δa |
|---|---|---|---|---|
| ALCOA | MT, 6.3 in. | 0.063 in.<br>0.125 in. | no | secant |
| FTA | MT, 12 in.<br>CT, 2 in. | 0.063 in.<br>0.125 in. | yes | DCPD,<br>unloading<br>compliance |
| FTI | MT, 9 in. | 0.063 in.<br>0.125 in. | no | secant |
| NASA LaRC | CT, 2 in.,<br>CT, 4 in. | 0.063 in.<br>0.125 in. | yes | unloading<br>compliance |
| UVA | CT, 3 in. | 0.125 in. | yes | DCPD |

## RESULTS AND DISCUSSION

In the following sections, stress intensity has been calculated by two methods. The secant analysis stress intensity, K-effective or $K_{eff}$, is determined by the instantaneous load and an effective crack length, $a_{eff}$. The effective crack length is determined by the secant compliance from the load-displacement curve (ASTM standard E-561). Stress intensity, K, calculated from J ($K_J$ hereafter) is determined by the following equation[3]:

$$K_J = (JxE)^{½} \quad (1)$$

The calculation of J is from ASTM standard E-1152 and requires measurement of the physical crack length, $a_{phys}$. Physical crack length may be measured by any of several methods including unloading compliance, direct current potential drop (DCPD), or visual measurement with a traveling microscope.

Figure 2 illustrates some of the terminology used in this report. The secant and elastic unloading compliances are used to determine the effective and physical crack

lengths respectively. Secant compliance and hence, $a_{eff}$, may be determined after test completion directly from the load displacement record. Elastic unloading compliance, on the other hand, must be determined at points on the load displacement curve as the curve is generated during the test. Stress intensity and compliance solutions for MT and CT specimens are detailed in the attached appendix.

### Wide Panel Tests

The wide panel test results were provided to NASA LaRC by Boeing in the form of load displacement curves and visually measured physical crack lengths. $K_J$-R and secant compliance based $K_{eff}$-R curves were generated from the load-displacement (P-$\delta$) curves and the physical crack length data. The $K_J$-R curves and the $K_{eff}$-R curves are shown in figures 3a and b respectively. Both analyses methods indicate that the crack growth resistance is greater in the 0.125 inch thick material than in the 0.063 inch thick material. This observed behavior may result from comparatively more buckling in the thinner panel reducing the load carrying capability of the panel, a hypothesis which is supported by the raw data load-displacement curves: Unloads on the B=0.063 in. P-$\delta$ curve show larger hysteresis loops than those on the B=0.125 in. P-$\delta$ curve. Figures 4a and b show $K_{eff}$ and $K_J$ plotted against the corresponding physical crack extension, $\Delta a_{phys}$. The figures indicate that both analysis methods yield essentially identical results. The same result is observed if $K_{eff}$ and $K_J$ are plotted against the effective crack extension, $\Delta a_{eff}$. Elastic stress intensity with no plasticity correction is also plotted for comparison. As expected, uncorrected elastic stress intensity significantly underestimates the crack driving force.[1]

### Middle Crack Tension (MT) Tests

Figures 5a and 5b show MT panel test data ($K_{eff}$ vs. $\Delta a_{eff}$) for 0.125 in. and 0.063 in. thick material respectively. Figure 5a indicates that 6.3 in., 9 in., and 12 in. wide panels give similar results at $\Delta a_{eff}$ up to approximately 1.2 inches; this is beyond the range of validity for all of the specimens. The stress intensity at maximum load, $K_C$, increases with increasing panel size. Figure 5b, 0.063 in. thick material, shows that the 6.3 in. and 12 in. wide MT panels provide similar results but the 9 in. panel data is different. In general, the data indicate good inter-laboratory reproducibility for K-R curves determined by the method of E-561, an exception being the 9 in. wide, 0.063 in. thick specimen.

Figure 6 compares the $K_{eff}$ vs. $\Delta a_{eff}$ R-curves for 6.3 in. and 12 in. wide MT specimens of 0.063 in. and 0.125 in. thick material. As was shown in figures 5a and 5b, the panel widths do not affect the R curve except at very large effective crack extension. At large crack extensions, the 6.3 in. R-curves bend sharply upward indicating full ligament plasticity. The data in figure 6 indicate higher R-curves for the 0.125 in. thick 2024-T3 than for the 0.063 in. thick material.

Figure 7 compares $K_J$ vs. $\Delta a_{phys}$ R-curves for 0.125 in. and 0.063 in. thick, 12 in. wide MT panels. When the data are presented in this manner, the difference

between the 0.125 in. and 0.063 in. thick material is reduced to an insignificant amount. Figure 8 compares the two analysis methods, $K_J$ and $K_{eff}$ for the 12 in. MT specimen with B = 0.125 in. Stress intensities are plotted against $\Delta a_{phys}$. As in figure 4b, it is shown that these two analyses provide equivalent results. Figure 9 is the same as figure 8 except that the results are for 0.063 in. thick material. The results presented in figures 6-9, indicate that in the absence of observable buckling, the 0.063 in. and 0.125 in. thick 2024-T3 exhibit identical R-curves when stress intensity is plotted as a function of $\Delta a_{phys}$. When stress intensity is plotted as a function of $\Delta a_{eff}$, the R-curves show some slight but consistent degree of separation, with the thicker material having the higher R_curve.

**Compact Tension (CT) Tests**

Figure 10 shows R-curves for W = 2 in., 3 in., and 4 in., B = 0.125 in., CT specimens tested at three different labs with $a_0/W$ ranging from 0.575 to 0.7. The data are plotted as $K_{eff}$ against $\Delta a_{eff}$. The R-curves for all of the specimens are very similar. This figure also points out one of the advantages of the advantages of the secant method as compare to methods which require measurement of physical crack length: The data for the W = 4 in. compact tension specimen, which could not be analyzed by E-1152 methodology because of inaccurate crack length measurement, was analyzed by the secant method (E-561) and the results were consistent with other test data.

Figure 11 shows $K_J$ vs. $\Delta a_{phys}$ for 2 in. and 3 in. W CT specimens with B = 0.063 in. and 0.125 in. All of the R-curves are similar, with the greatest spread between the 0.063 in. thick specimen test results. Figure 12 again shows the equivalence between $K_J$ and $K_{eff}$, this time in W = 2 in., B = 0.063 in. and 0.125 in. CT specimens. This figure also indicates that there is very little difference in the R-curve behavior of the two thicknesses of 2024-T3 in this specimen configuration. Figure 13 shows the same stress intensity data crack extension. Plotted in this way, the data for the 0.063 in. and 0.125 in. thick material converge at much higher crack extensions.

**Comparison Between Specimen Types**

Figure 14 shows $K_{eff}$ against $\Delta a_{eff}$ R-curves for a W = 2 in. CT and a W = 12 in. MT, both at B = 0.063 in. The correspondence between the two curves is not very good. Figure 15 is a similar plot for 0.125 in. thick specimens. The R-curves in figure 15 exhibit less separation than those in figure 14. Figures 16 and 17 are identical to figures 14 and 15 except that the plotted stress intensities are calculated from J and they are plotted as a function of physical crack extension. In figures 16 and 17 one can see that the correspondence between the W = 2 in. CT and W = 12 in. MT R-curves is quite good. The MT curves are somewhat ragged because, at low crack length, MT specimens are very stiff and clip gages with high sensitivity (and therefore high noise levels) are required to measure crack length. Figures 14-17 indicate that

better data correspondence between specimen types is obtained by plotting either $K_J$ or $K_{eff}$ against physical crack extension compared to a plot of stress intensity against effective crack extension.

### Comparison Between Wide Panels and Small Specimens

The best comparisons between small specimens and the wide panel test results are made with the MT specimens. This is because larger crack extensions are measured in the MT specimens, allowing comparison over a greater portion of the R-curve than is possible with the CT specimens. Because all of the MT test results were similar (with the exception of the W = 9 in., B = 0.063 in. specimen), only the 12 in. wide MT panels will be used for comparison. These were also the only MT specimens for which adequate $\Delta a_{phys}$ data for J analyses were obtained.

Figure 18 illustrates the excellent correspondence between the B = 0.063 in., 12 in. wide MT panel and 60 in. wide panel, $K_J$ vs. $\Delta a_{phys}$ R-curves. In figure 19, the results from the same tests are plotted as $K_{eff}$ against $\Delta a_{eff}$ and the correspondence is not as good; the 12 in. MT data is significantly below that of the 60 in. wide panel.

The comparison between 12 in. and 60 in. wide panels of 0.125 in. thick material is somewhat different. figure 20 is the same as figure 18 except that the data is for 0.125 in. thick material. The R-curves for the W = 12 in. and W = 60 in. panels are parallel but, the 12 in. wide panel data has a nearly constant negative offset of several ksi$\sqrt{in}$ from the wide panel data. The reason for this offset is not apparent. Figure 21 shows $K_{eff}$ against $\Delta a_{eff}$ for the 12 in. wide panel and the 60 in. wide panel. In this plot, the comparison between the 12 in. wide panel and the 60 in. wide panel appears to be quite good after the first 0.6 inches of effective crack extension. As was shown previously in figures 4b and 8, the $K_{eff}$ and $K_J$ at any given $\Delta a_{phys}$ or $\Delta a_{eff}$ are nearly the same for either the 60 inch wide panel or the 12 inch wide panel. This suggests the possibility of a slight error in the measurement of the physical crack extension of the 60 in. wide panel. An offset of several hundredths of inches (in a total crack length of greater than 8.8 inches) is all that would be required to cause the observed separation between the two curves in figure 19.

### Crack Length Measurement: Unloading Compliance and DCPD

Direct current potential drop and unloading compliance techniques give nearly identical crack length results. This is illustrated in figure 22, where $K_J$-R curves determined by DCPD and unloading compliance on the same specimen are compared. There may be some advantage to using DCPD on stiff specimens such as MT's which provide low sensitivity for compliance measurements. When specimen stiffness is high (compliance is low), the signal to noise ratio of the clip gage output will be low. This situation, which can be observed in figure 16, results in some uncertainty in crack length measurement and a generally "ragged" appearance to the R-curve at low crack extensions.

### Specimen Validity Limits

All of the MT and CT specimens are beyond their limits of validity before maximum load is attained therefore; any calculated $K_C$ or $K_{app}$ values will be invalid. All of the CT specimens are invalid, based on E-561, at low stress intensity, typically $< 41$ ksi$\sqrt{}$in. The validity criterion for CT specimen data is:

$$b \geq (4/\pi) \times (K/\sigma_{ys})^2 \qquad (2)$$

Where b is the un-cracked ligament and $\sigma_{ys}$ is the 0.2% offset yield strength. Figure 23 shows the regions of valid and invalid data for a W = 2 in. CT specimen. Plotted in figure 24 are the CT data from figure 23 and valid and invalid data from a 12 in. wide MT specimen. Figure 24 shows that there is good correspondence between the invalid CT data and the valid MT data well beyond the region of CT specimen validity, indicating the restrictions on validity of CT specimen data may be too severe.

For the MT specimen, ASTM standard E-561 specifies a validity criterion of net section stress, based on **physical crack length**, $< \sigma_{ys}$. An alternative criterion for data validity, used by one of the program participants is net section stress $< 0.8\sigma_{ys}$ based on **effective crack length**. An example of the restrictiveness of this validity criteria is shown in figure 25. In figure 25, the open circles represent the valid data based on net section stress less than 80% of the yield stress and net section calculated based on $a_{eff}$, if the net section stress is based on $a_{phys}$, then the filled circles are also valid data. If the ASTM criterion of net section stress greater than 100% of the yield stress is used, then even more data can be considered valid. Based on the $a_{eff}$ criterion, net section stresses in the un-cracked ligament of a 6.3 in. wide MT specimen were calculated to be as high as 150 ksi. Of course, calculation of $\sigma_{net}$ based on physical crack length requires measurement of physical crack length.

## CONCLUDING REMARKS

Several notable observations may be made as a result of analysis of the R-curve data generated in the course of this program:

1. There is an excellent correlation between $K_J$ and $K_{eff}$. This correlation casts some doubt on the necessity for complicated J calculation and test procedures when producing R-curves for 2024-T3. For higher strength or lower toughness alloys, J based analysis will be less useful than for 2024-T3.

2. Secant analysis R-curve testing is very simple to perform and appears to give good data; however, there are good reasons for J-based testing and in particular for physical crack length measurement.

   a. Data indicate that better correlation between specimen types is obtained when $K_J$ or $K_{eff}$ are plotted against $\Delta a_{phys}$ rather than $\Delta a_{eff}$ (see figures 14-17).

   b. Net section stresses in MT tests should be based on true net sections in order to make reasonable assessments of ligament plasticity; therefore, physical crack length measurements should be performed.

c. Careful application of ASTM standard E-1152 allows estimation of $J_{IC}$ hence $K_{IC}$ from R-curve tests.

3. The useful range of CT derived R-curve data appears to extend well beyond the validity limits set in E-561. Careful comparison between invalid CT specimen and valid MT specimen data from several different alloys should show whether this is a general concurrence.

## REFERENCES

1. ASTM Standard E 561-86, "Standard Practice for R-Curve Determination", 1991 Annual Book of ASTM Standards, vol. 3.01, pp. 577-588.
2. ASTM Standard E 1152-87, "Standard Test Method for Determining J-R Curves", 1991 Annual Book of ASTM Standards, vol. 3.01, pp. 825-835.
3. Anderson, T. L., Fracture Mechanics: Fundamentals and Applications, CRC Press, Boca Raton, Florida, pg. 141.

## APPENDIX

### Stress Intensity Solutions

1. Compact Tension (CT) Specimens:

$$K=\left(\frac{P}{BW^{1/2}}\right)*f\left(\frac{a}{W}\right)$$

$$f\left(\frac{a}{W}\right)=\frac{\left(2+\frac{a}{W}\right)}{\left(1-\frac{a}{W}\right)^{\frac{3}{2}}}\left[0.866+4.64\left(\frac{a}{W}\right)-13.32\left(\frac{a}{W}\right)^2+14.72\left(\frac{a}{W}\right)^3-5.6\left(\frac{a}{W}\right)^4\right.$$

2. Middle Crack Tension (MT) Specimens:

$$K=\left(\frac{P}{BW^{1/2}}\right)*f\left(\frac{a}{W}\right)$$

$$f\left(\frac{a}{W}\right)=\sqrt{\frac{\pi a}{4W}\sec\frac{\pi a}{2W}}\left[1-0.025\left(\frac{a}{W}\right)^2+0.06\left(\frac{a}{W}\right)^4\right]$$

## Compliance Solutions

1. Compact Tension (CT) Specimens:

$$\frac{a}{W} = 1.00196 - 4.06319U + 11.242U^2 - 106.043U^3 + 464.335U^4 - 650.677U^5$$

2. Middle Crack Tension (MT) Specimens:

$$\frac{2a}{W} = -0.01919 + 4.45932U + 21.4413U^2 - 145.73039U^3 + 241.77972U^4 - 128.845$$

where:

$$U = \frac{1}{\sqrt{\frac{BE\delta}{P} + 1}}$$

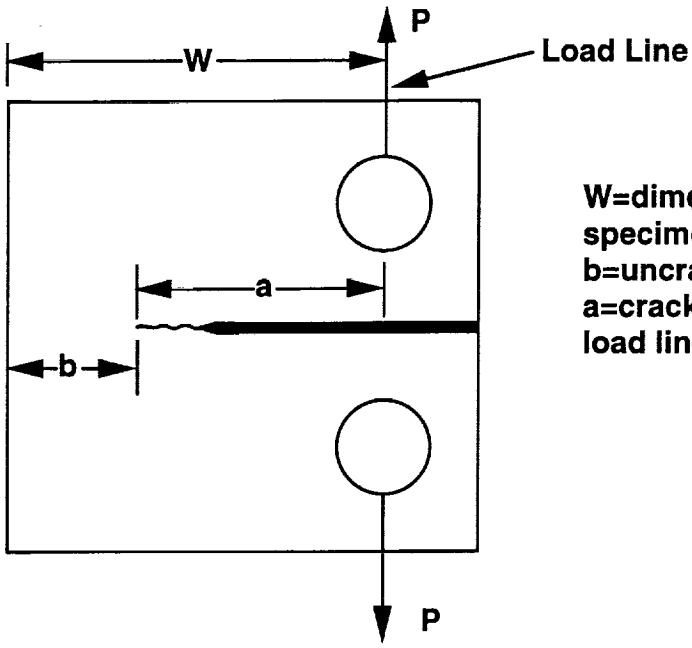


a) Compact Tension Specimen

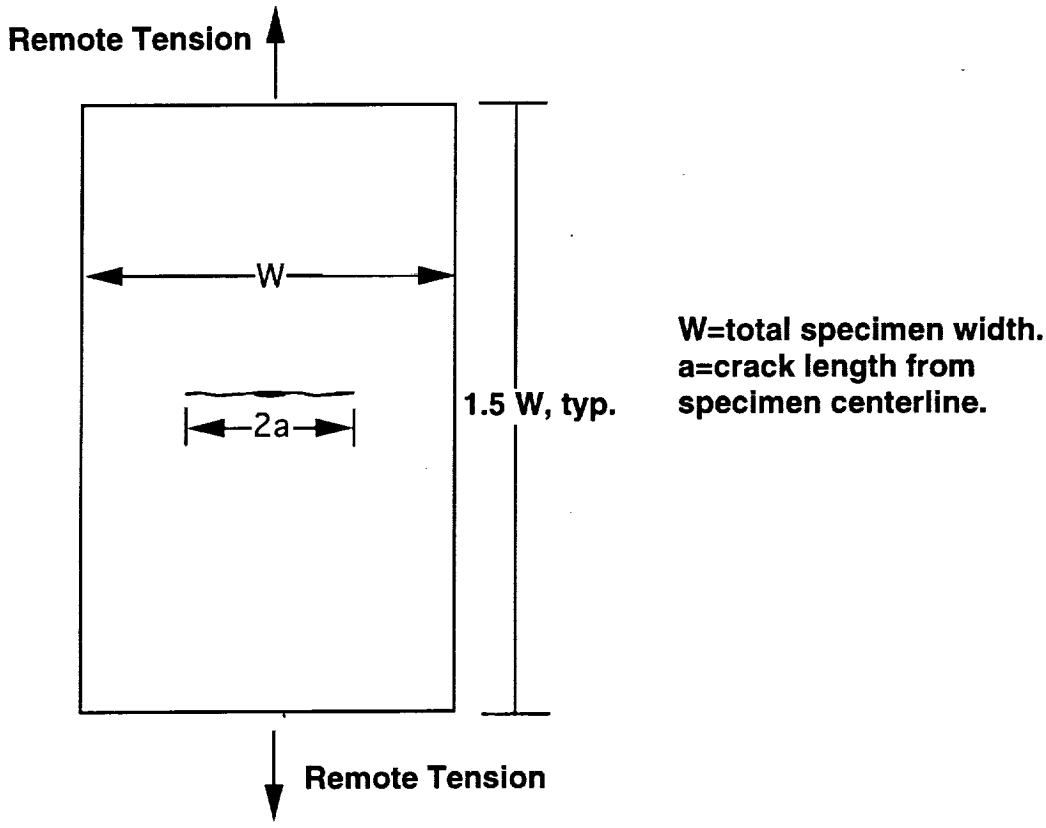


b) Middle Crack Tension Specimen



Figure 1. Specimen configurations used in fracture toughness tests.

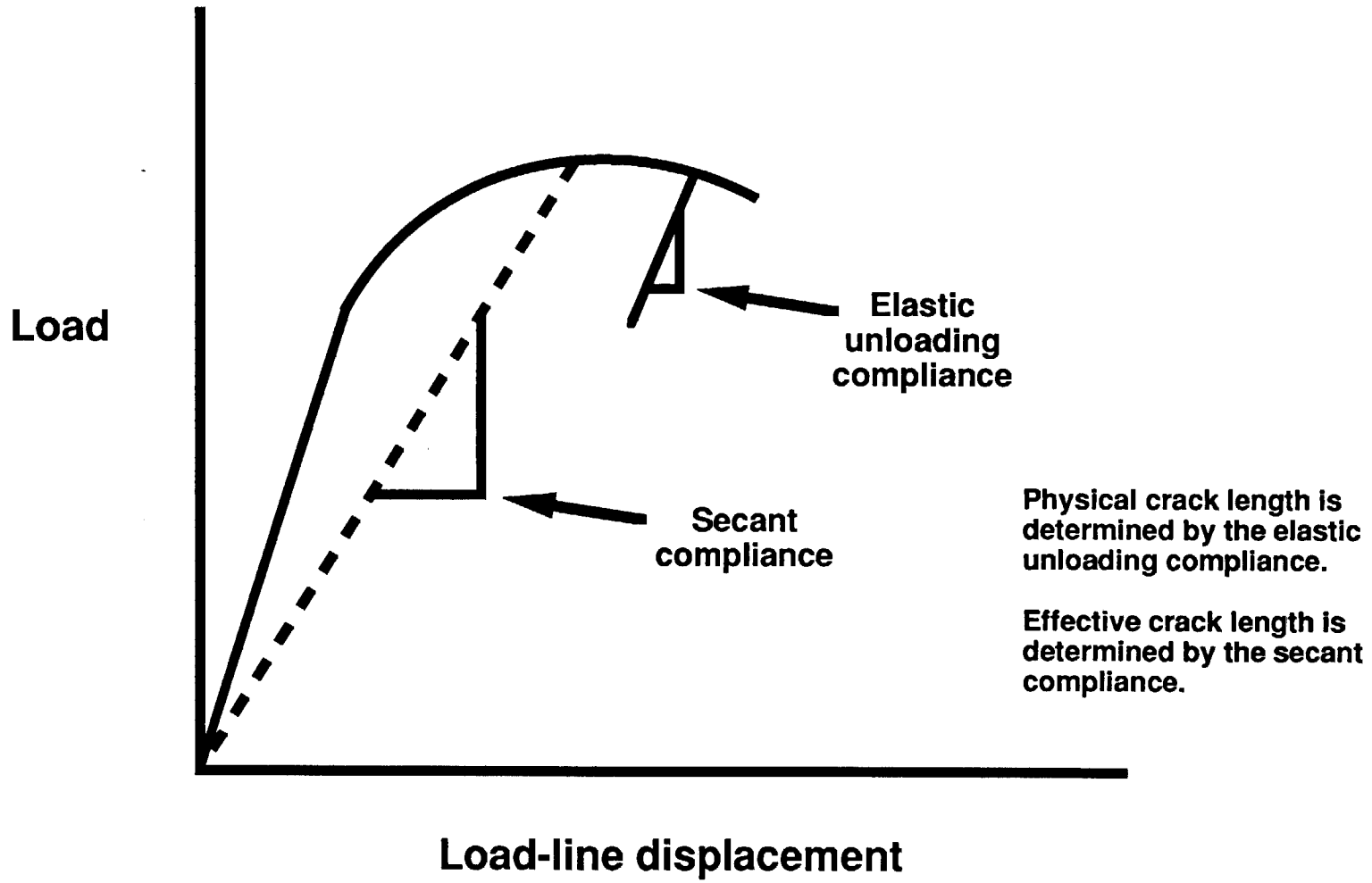


**Figure 2. Schematic Load vs. Load-line displacement curve.**

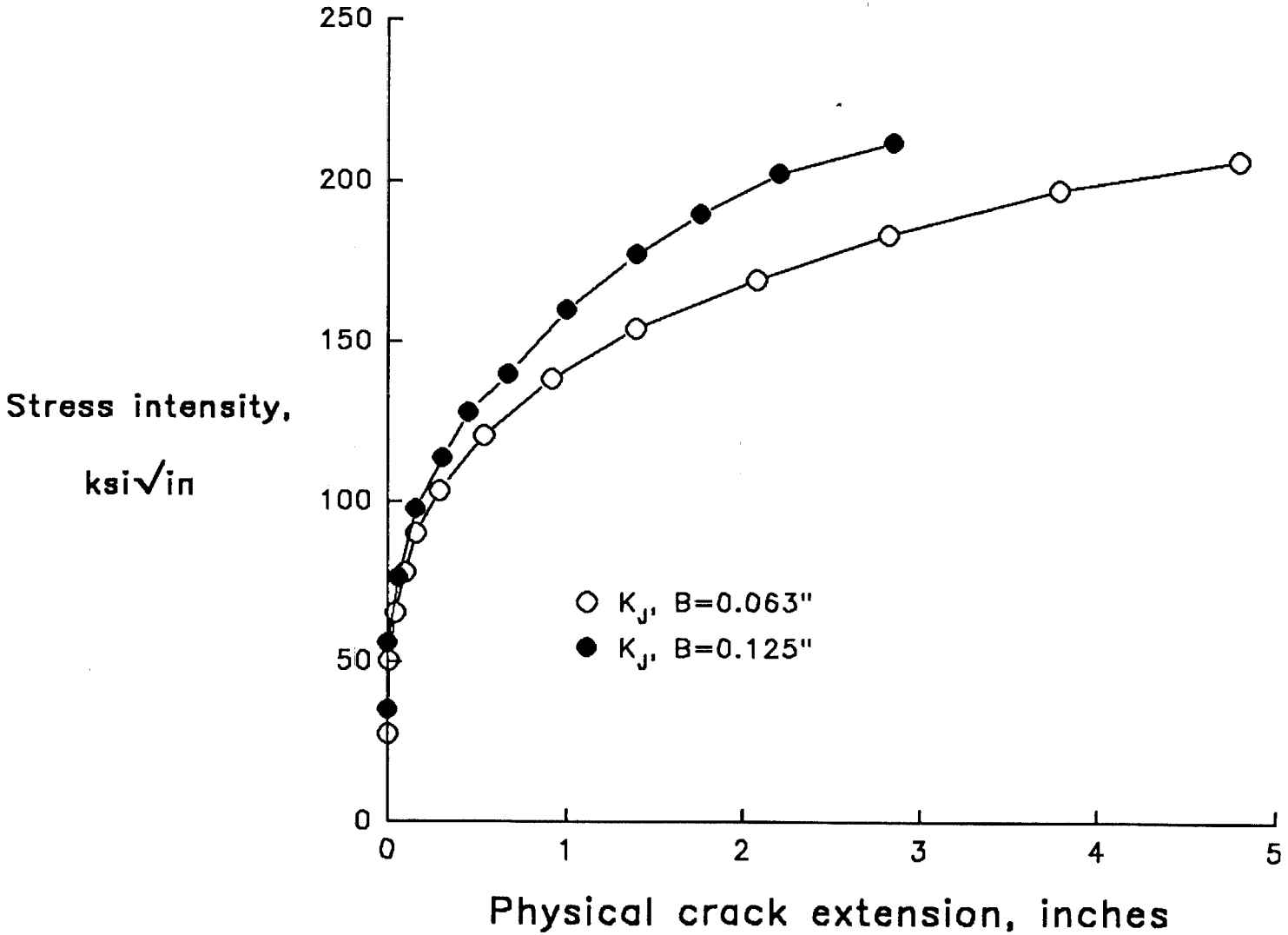


Figure 3a. MT Panel K–R curves, W=60 inches.

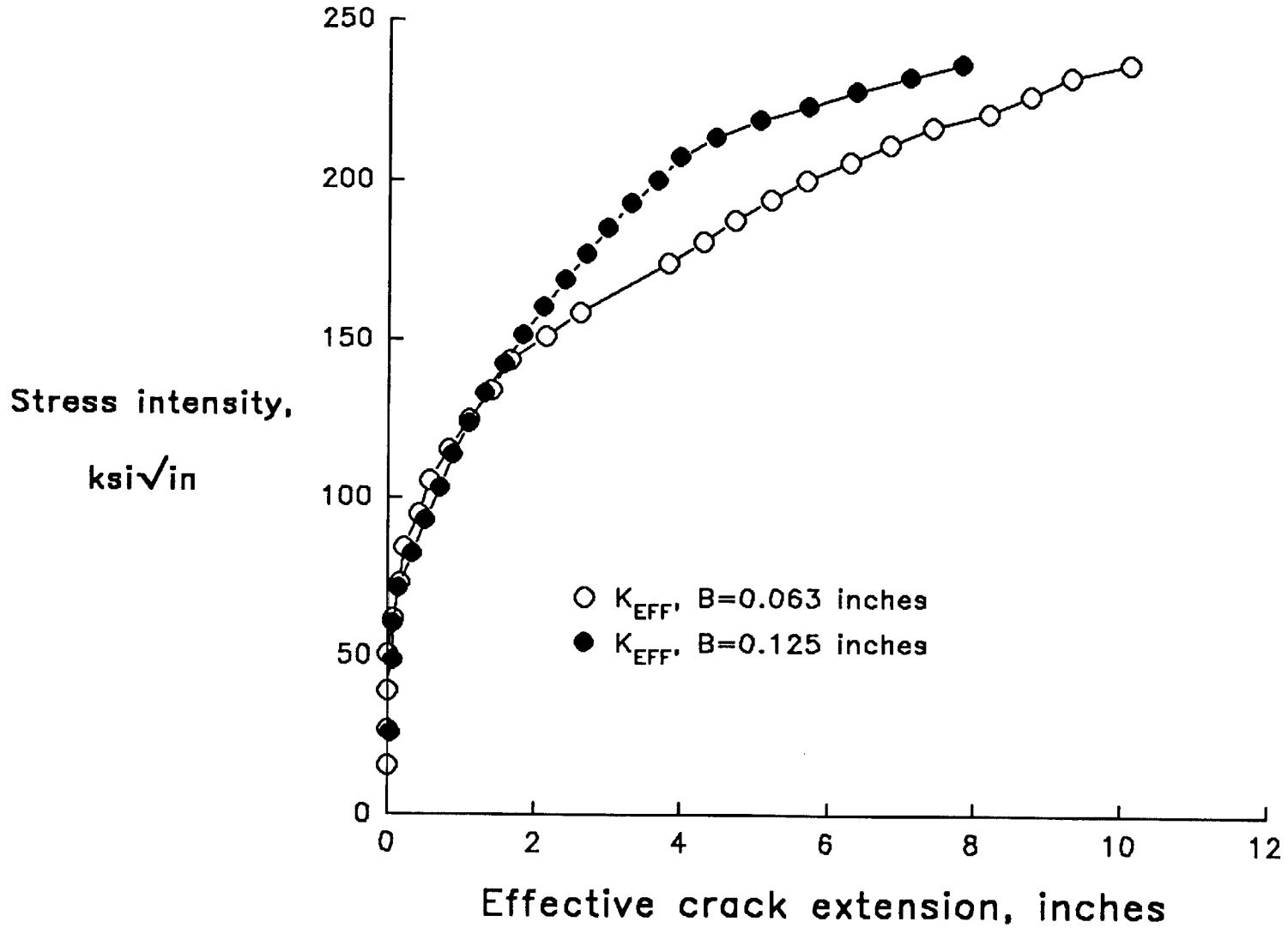


Figure 3b. MT panel K–R curves, W=60 inches.

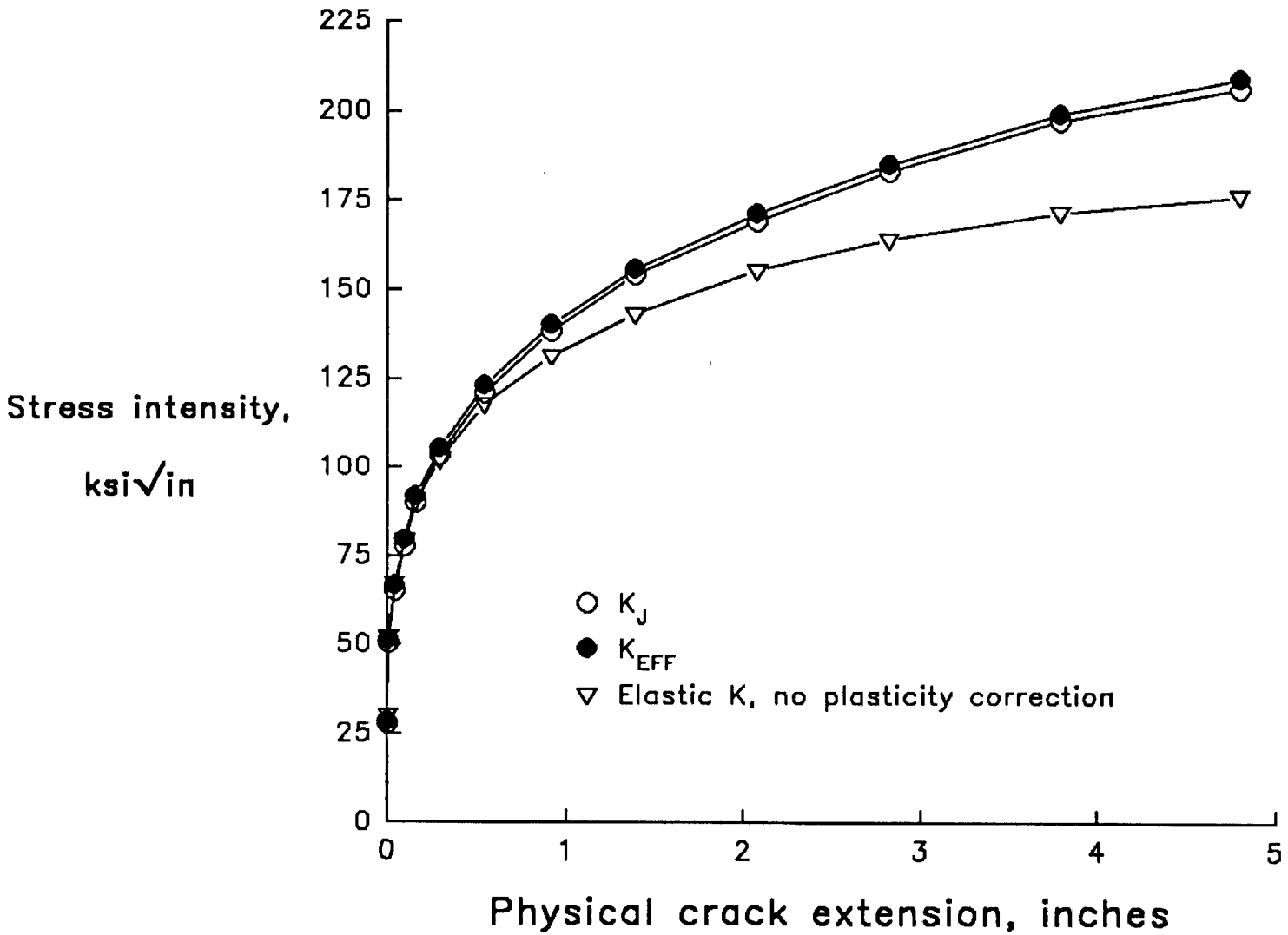


Figure 4a. MT panel K–R curves, W=60 inches, B=0.063 inches.

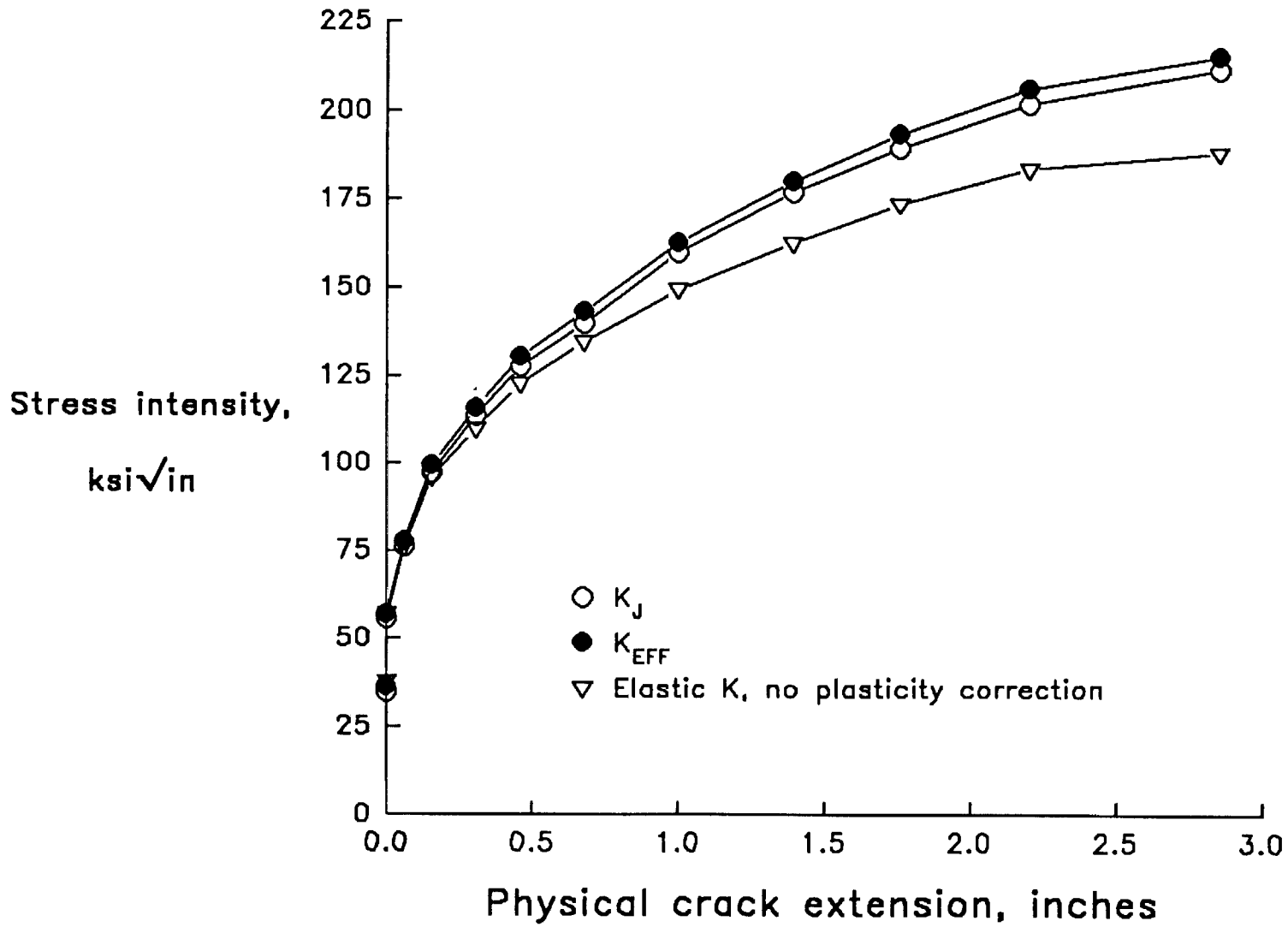


Figure 4b. MT panel K–R curves, W=60 inches, B=0.125 inches.

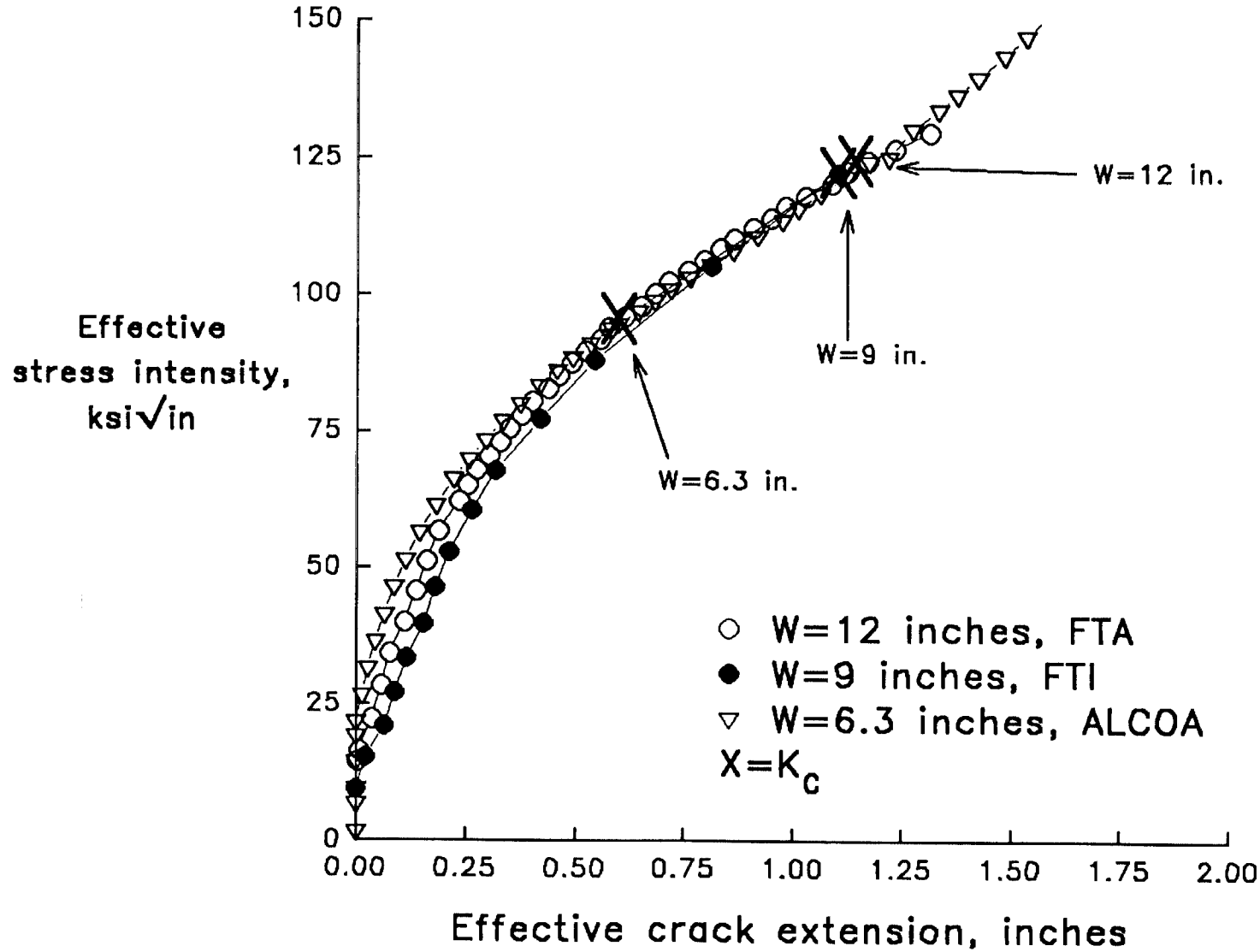


Figure 5a. MT specimen K–R curves, B=0.125 inches.

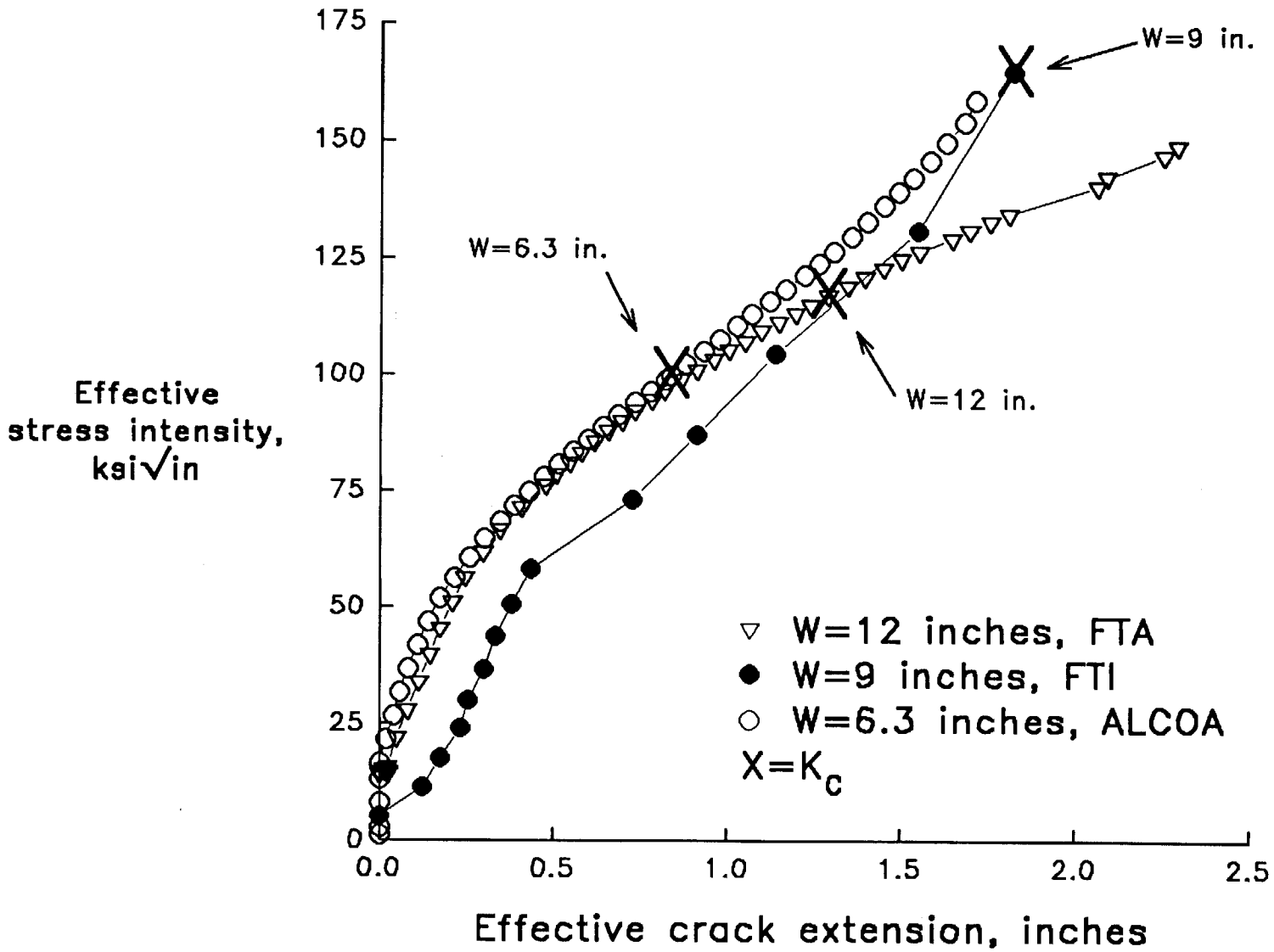


Figure 5b. MT specimen K–R curves, B=0.063 inches.

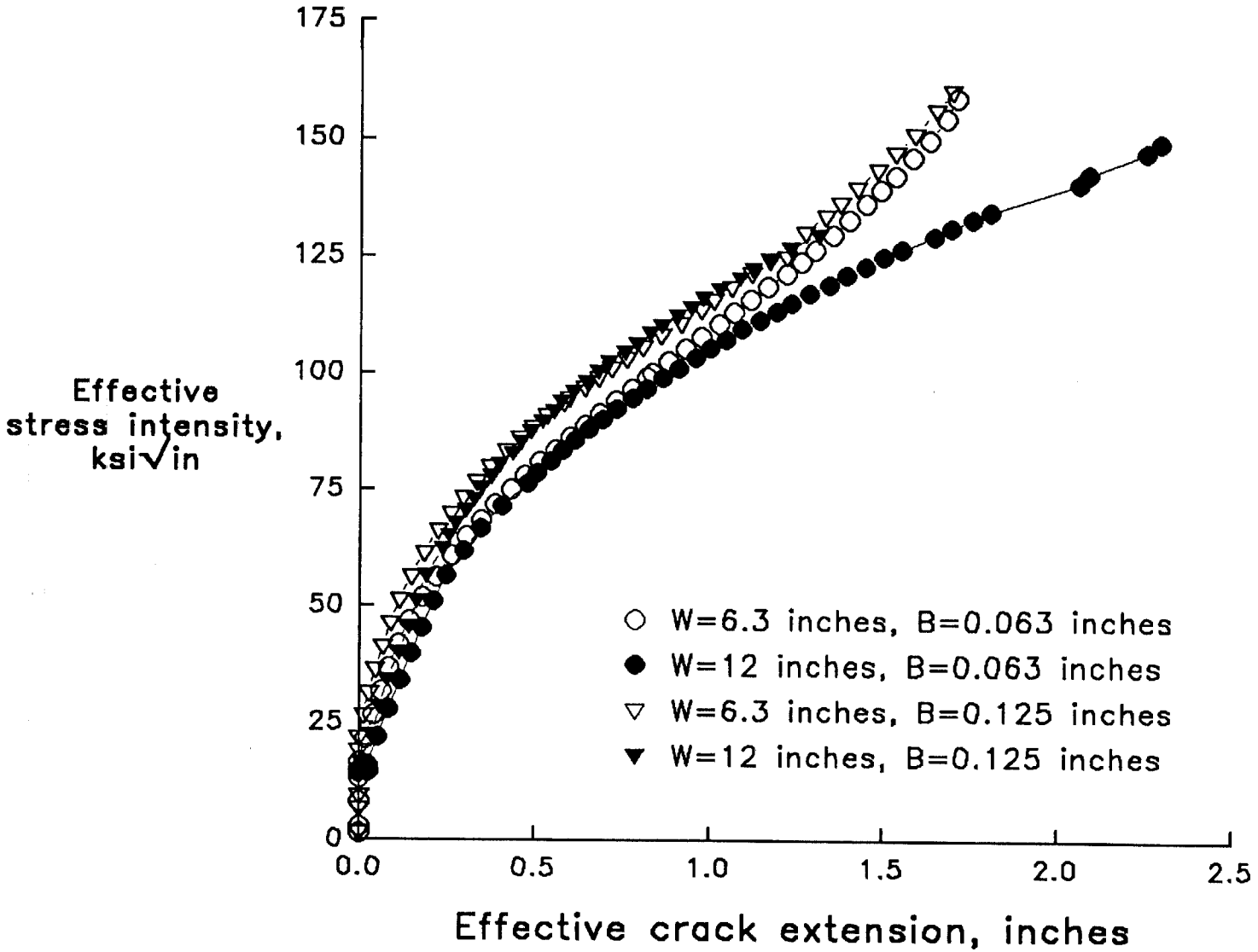


Figure 6. MT panel K–R curves.

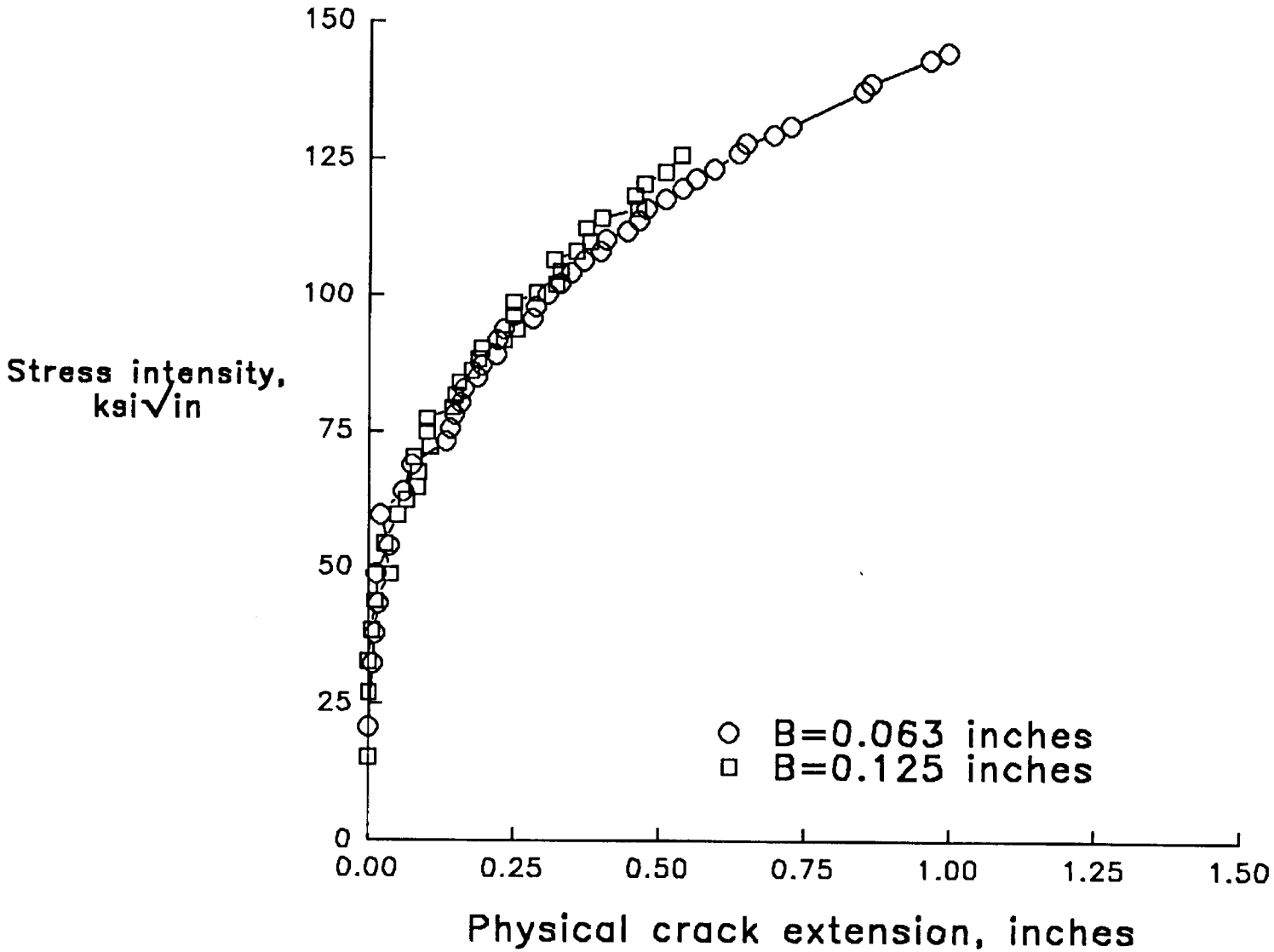


Figure 7. MT panel $K_J$–R curves, W=12 inches.

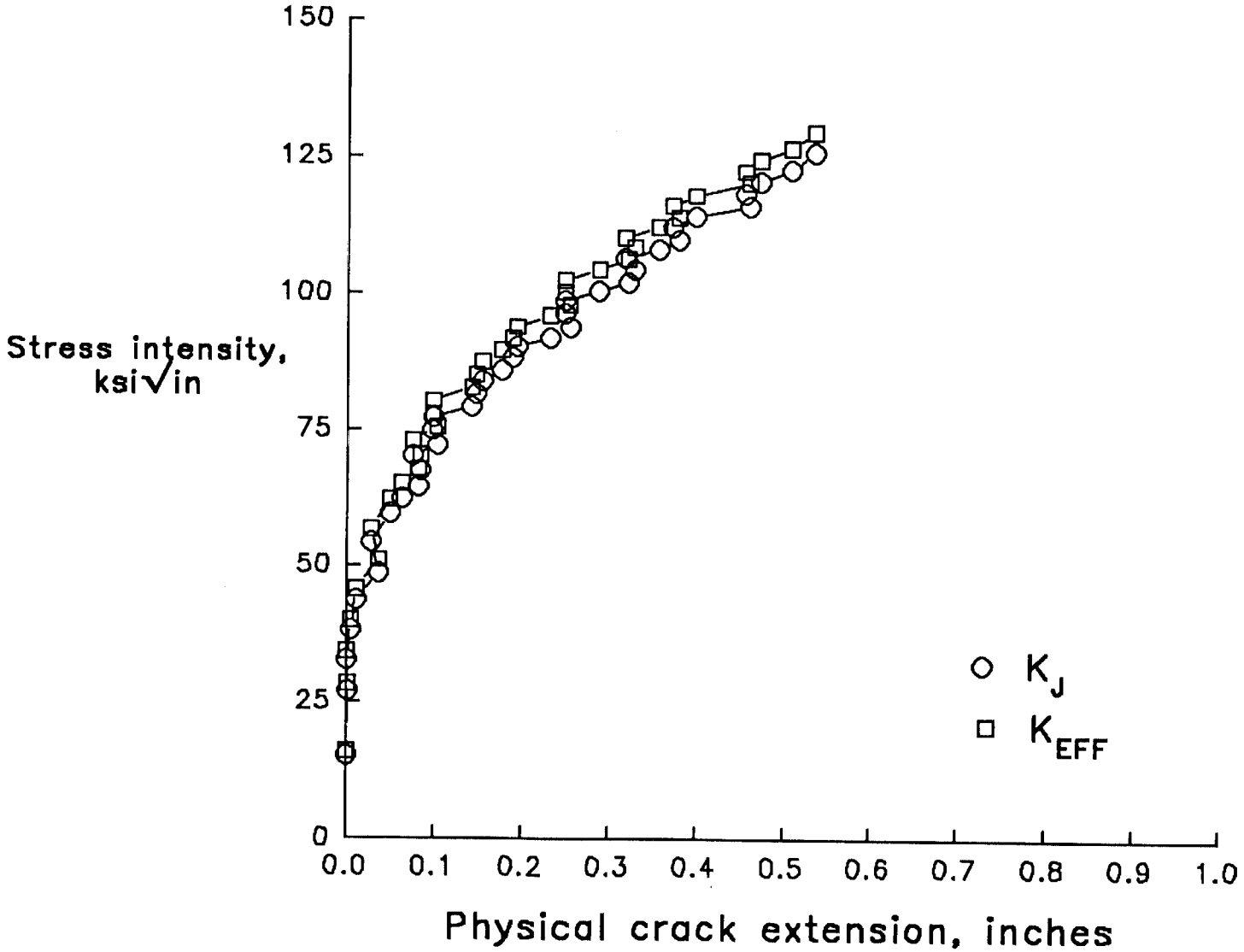


Figure 8. MT panel K–R curves, W=12 inches, B=0.125 inches.

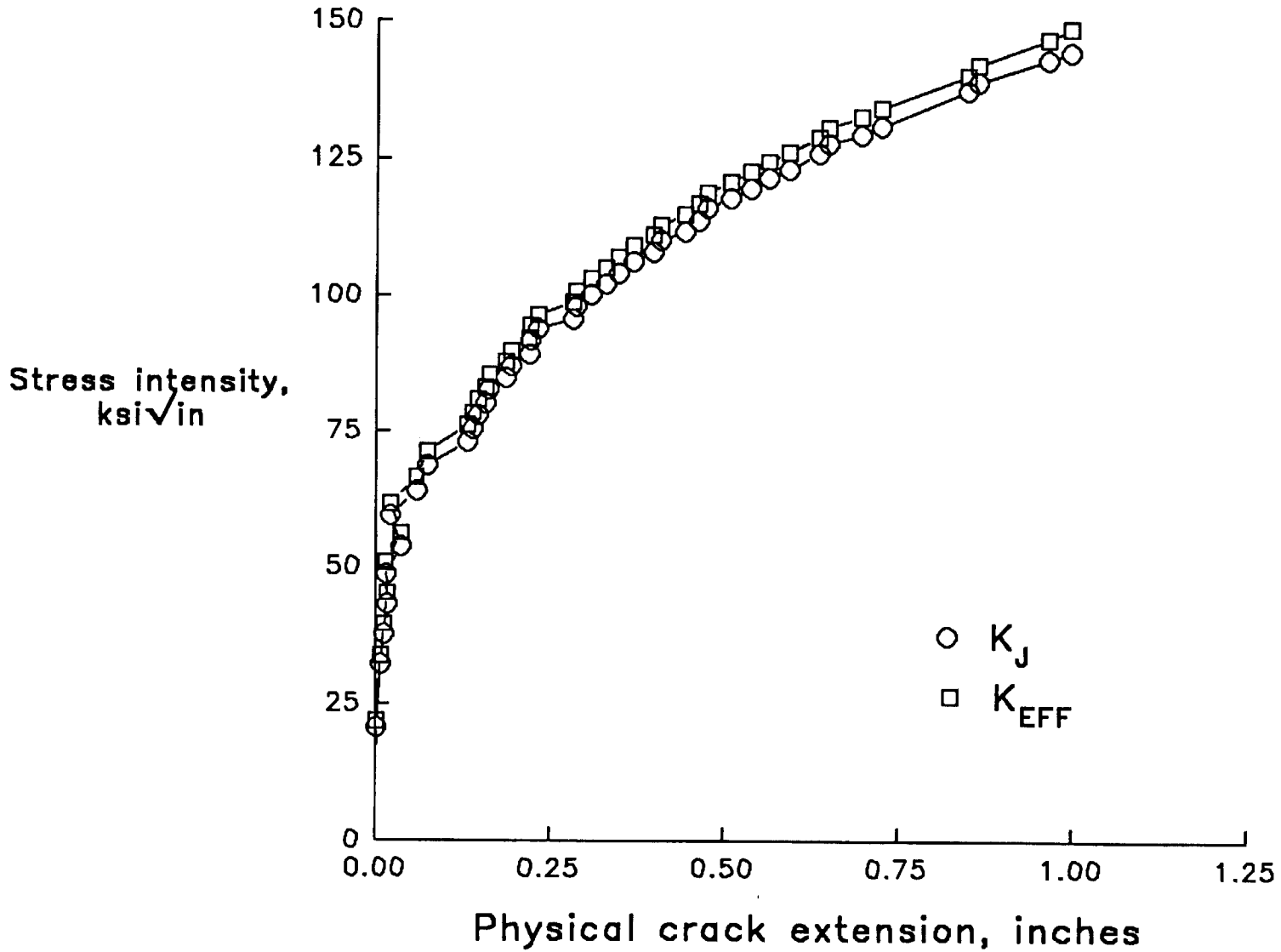


Figure 9. MT panel K–R curves, W=12 inches, B=0.063 inches.

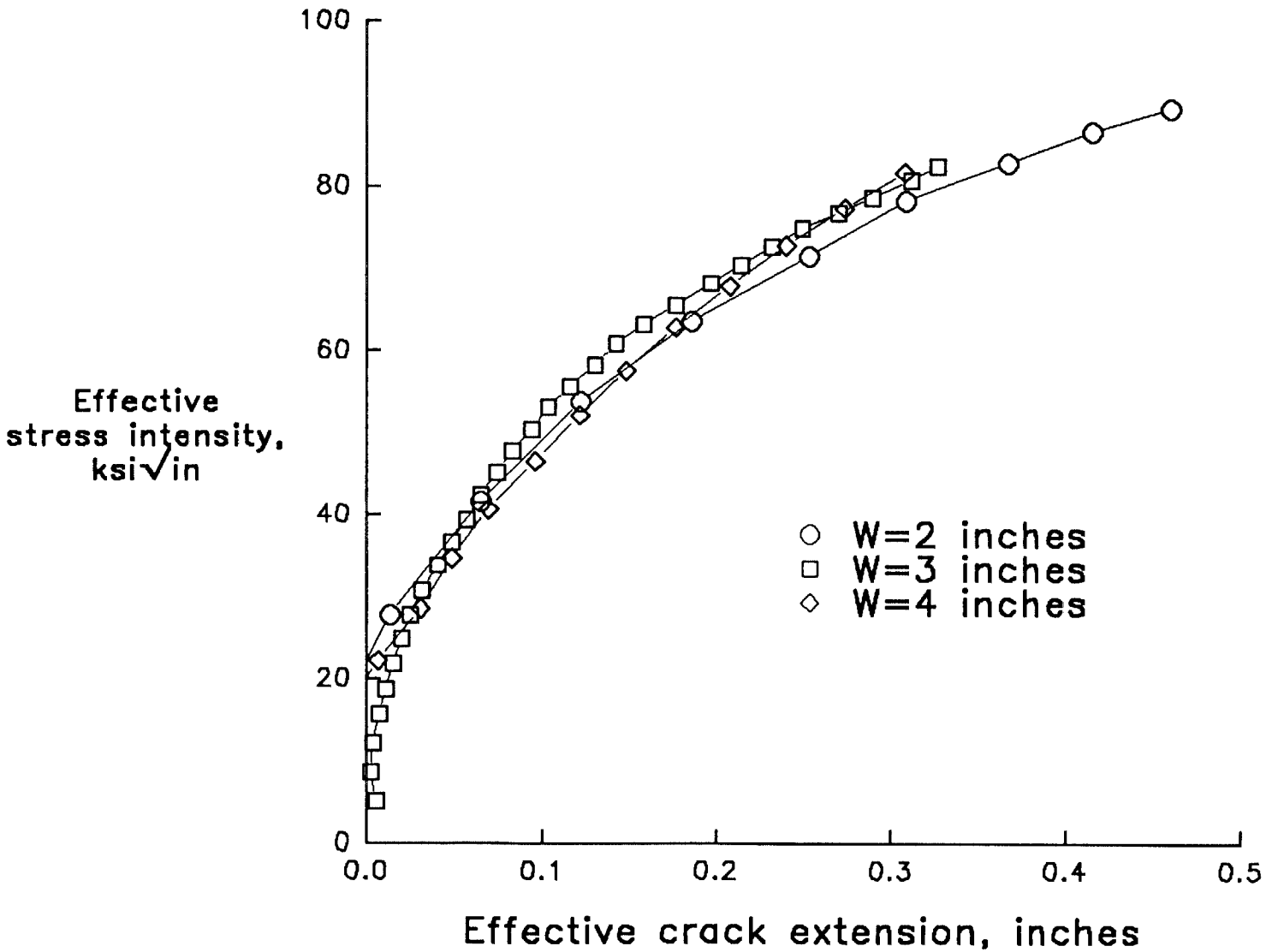


Figure 10. CT specimen $K_{EFF}$–R curves, B=0.125 inches

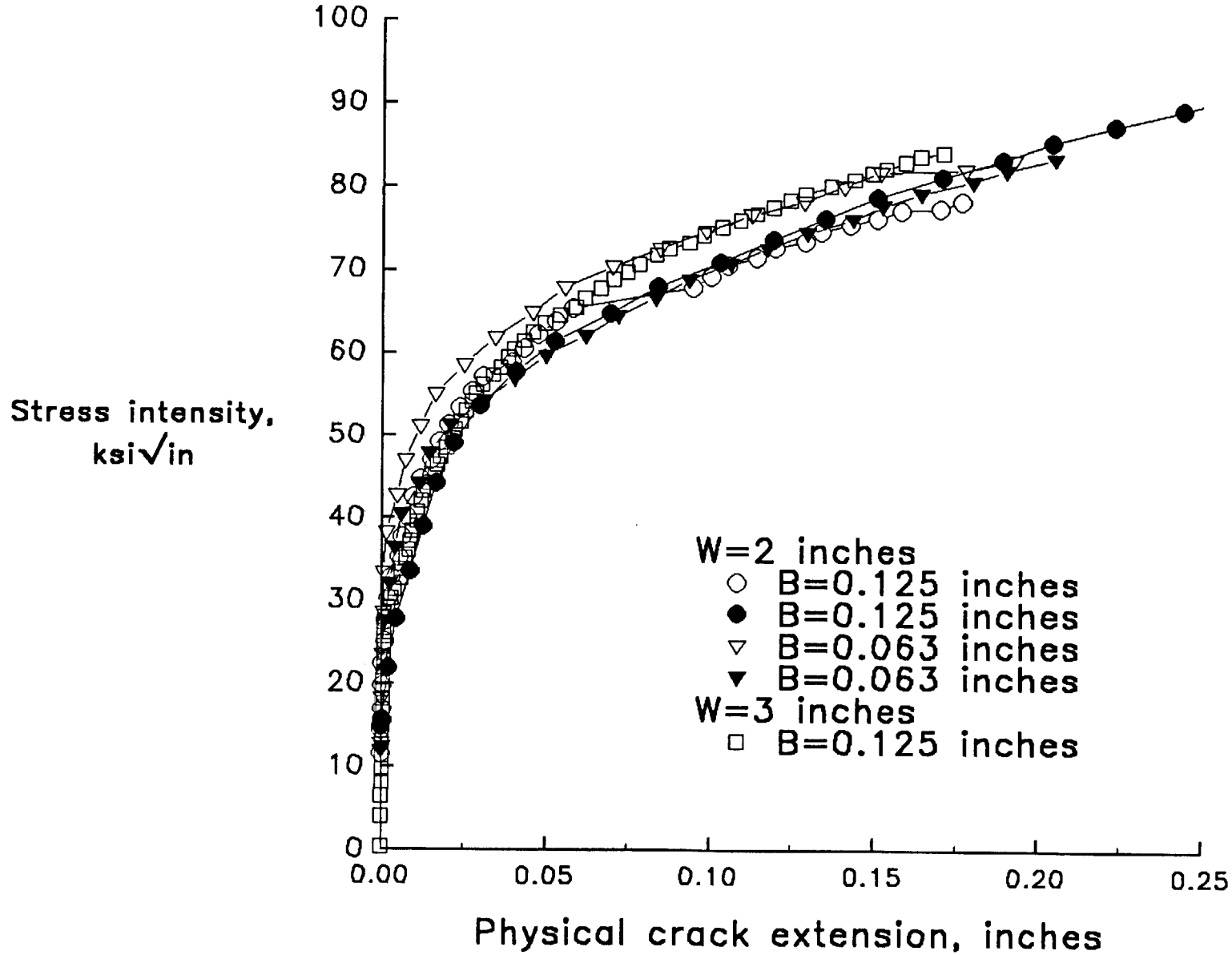


Figure 11. CT specimen $K_J$–R curves.

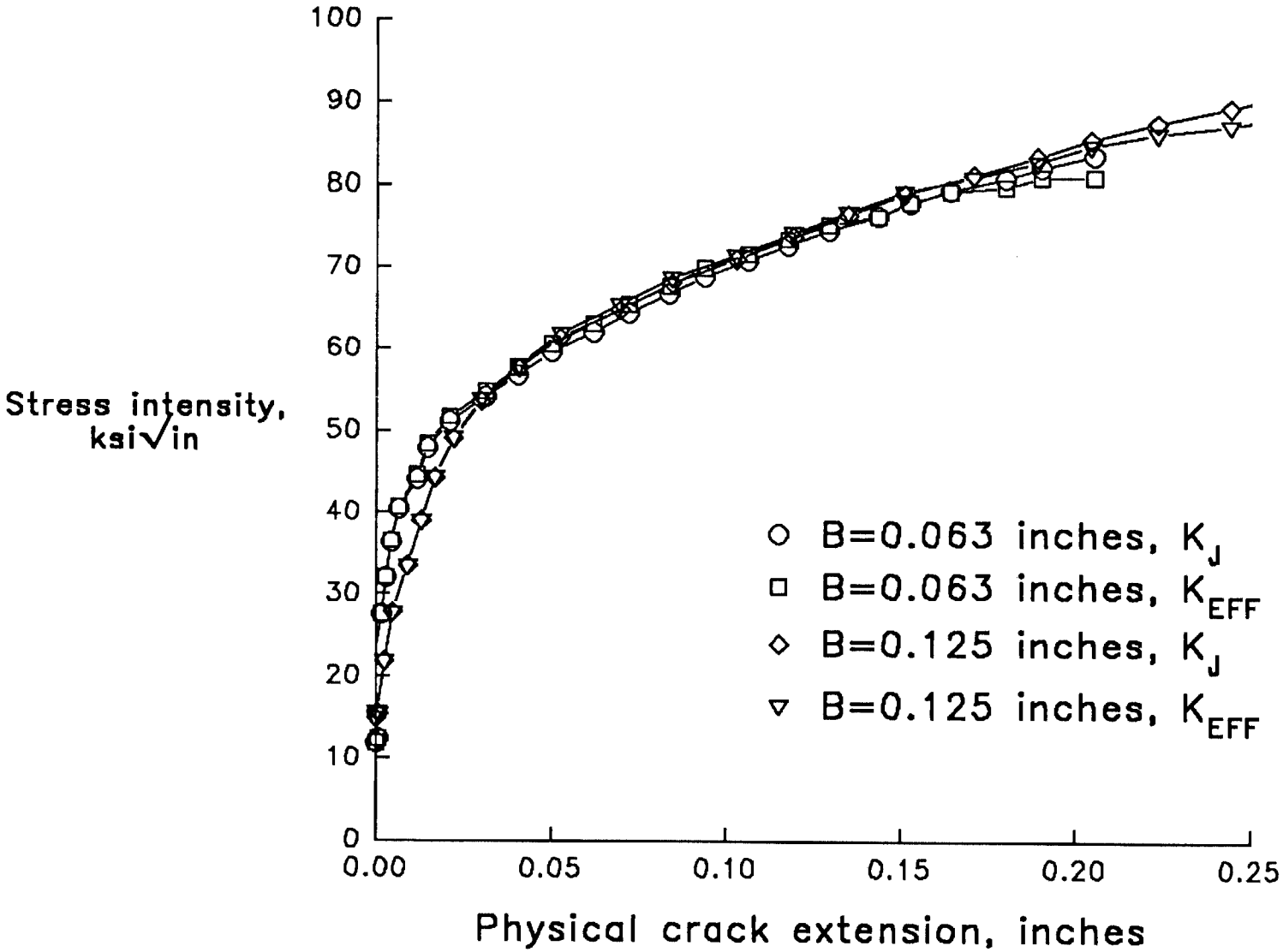


Figure 12. CT specimen K–R curves, W=2 inches.

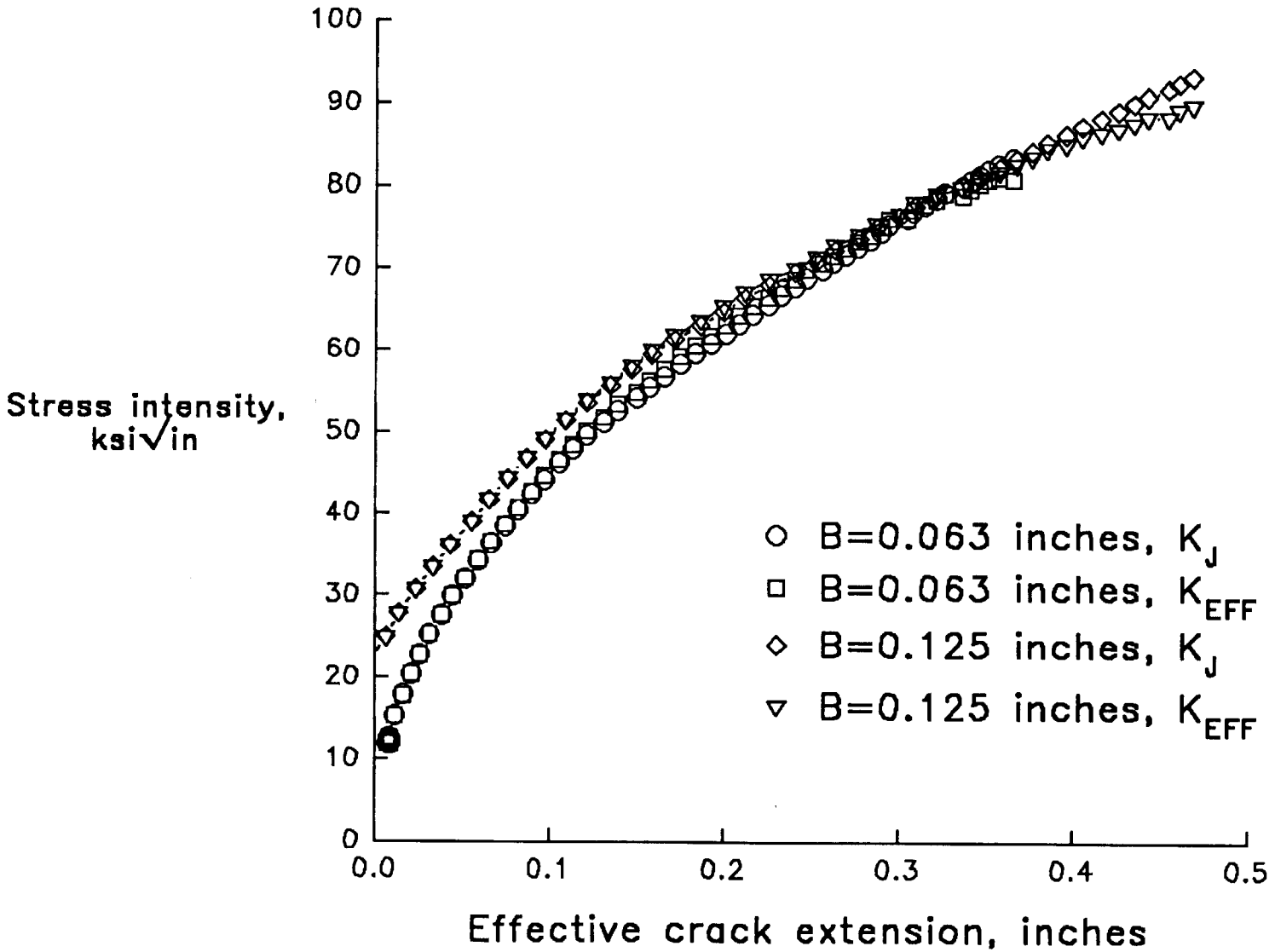


Figure 13. CT specimen K–R curves, W=2 inches.

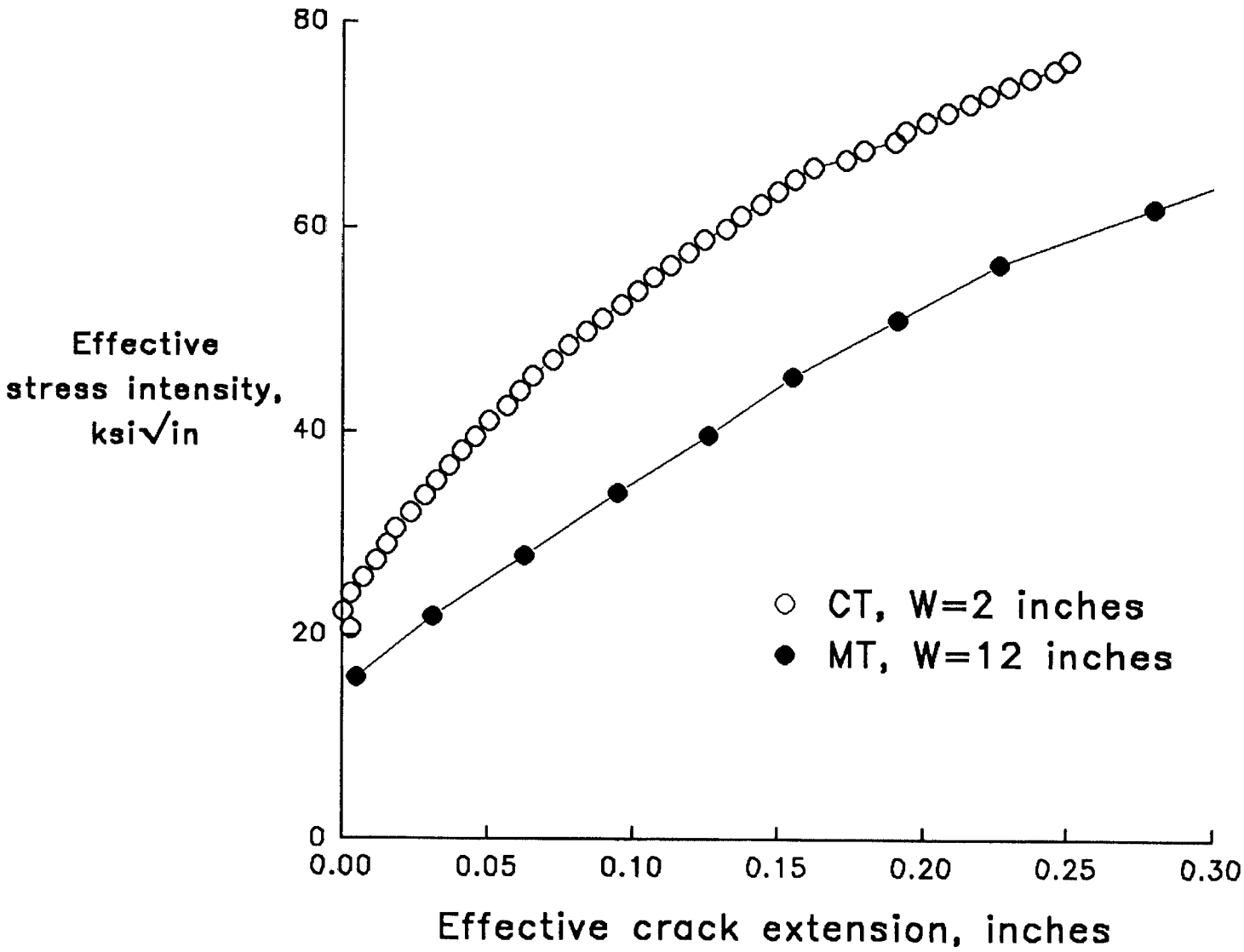


Figure 14. $K_{EFF}$–R curves, B=0.063 inches.

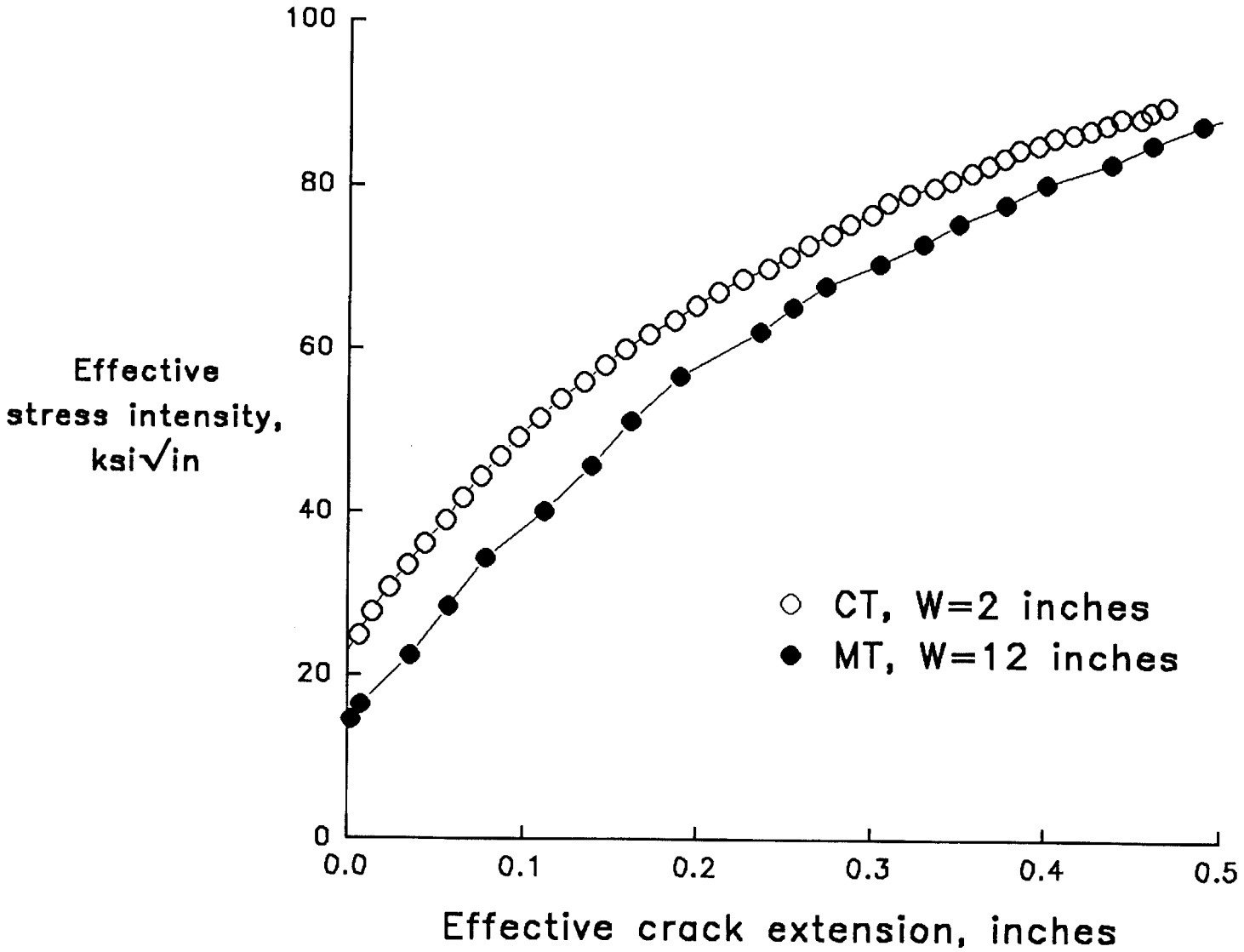


Figure 15. $K_{EFF}$–R curves, B=0.125 inches.

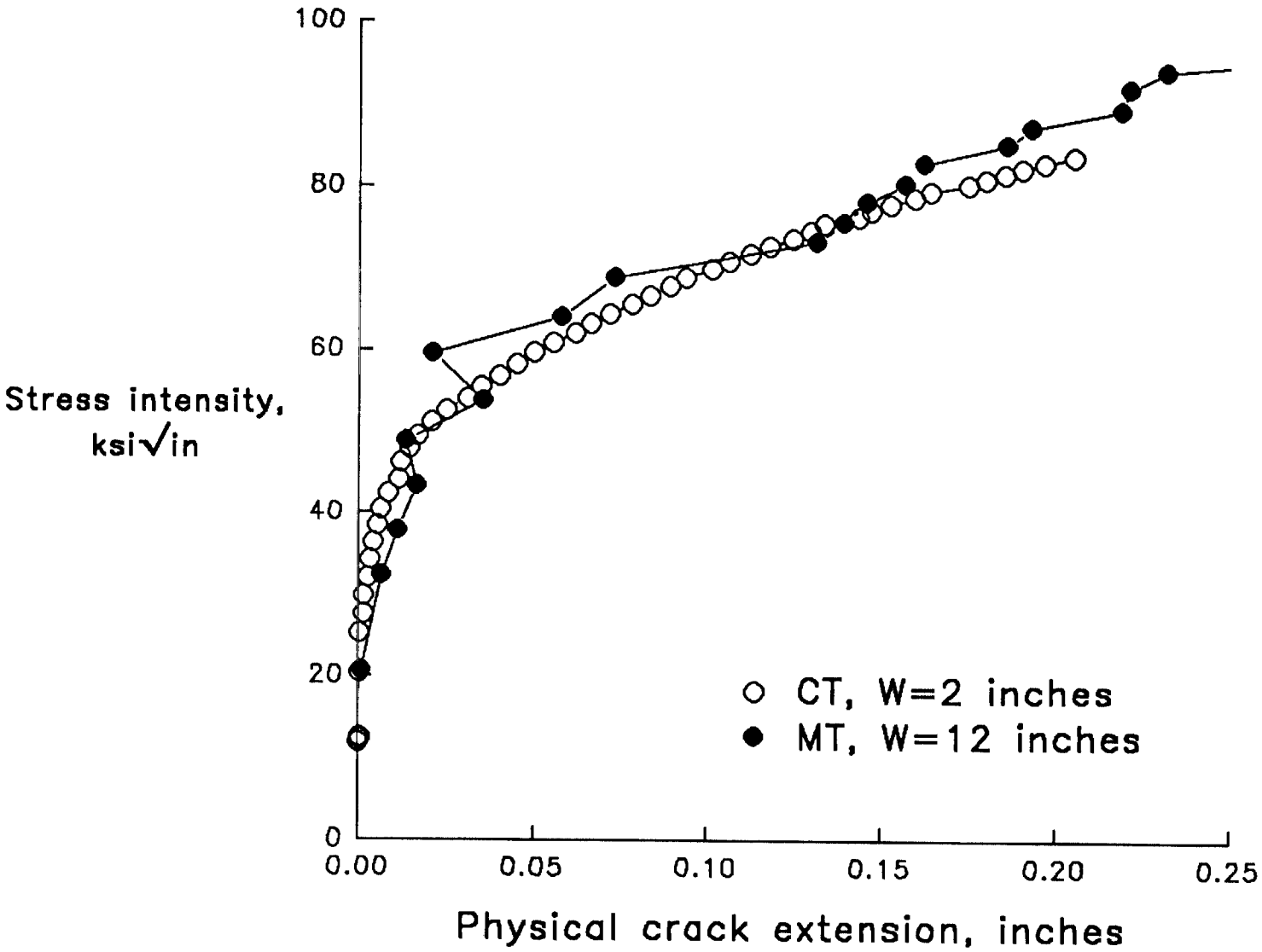


Figure 16. $K_J$–R curves, B=0.063 inches.

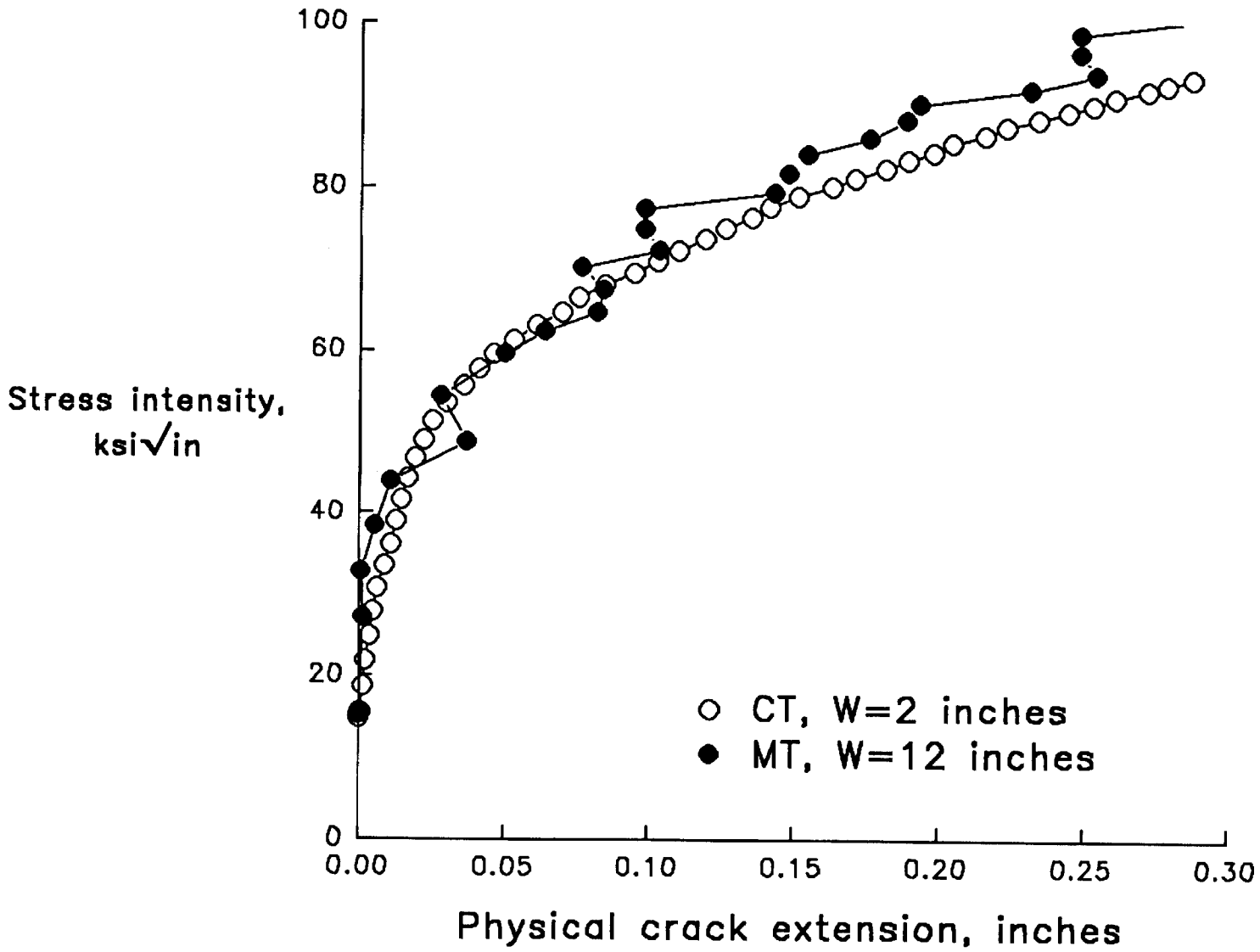


Figure 17. $K_J$–R curves, B=0.125 inches.

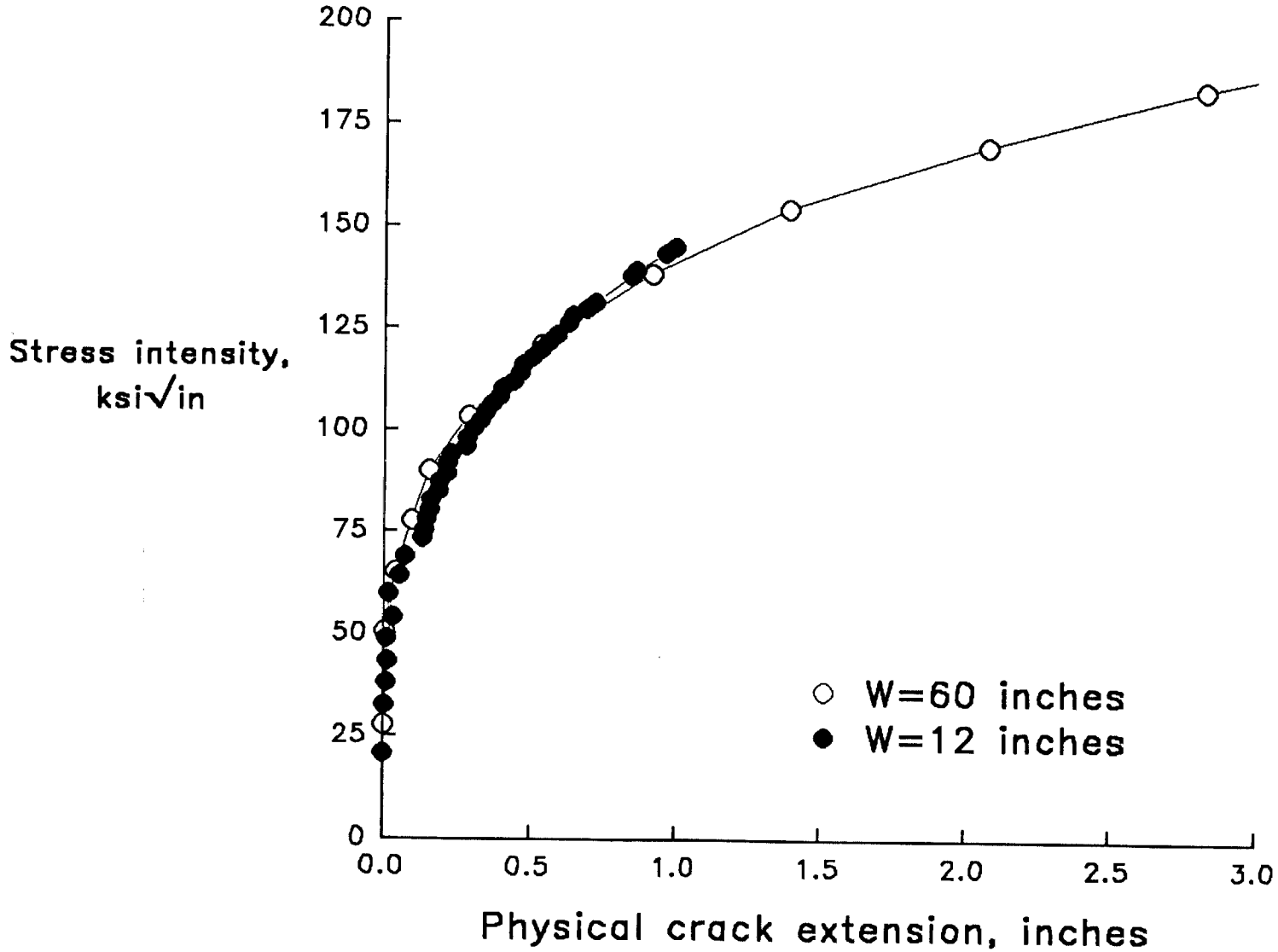


Figure 18. MT panel $K_J$–R curves, B=0.063 inches.

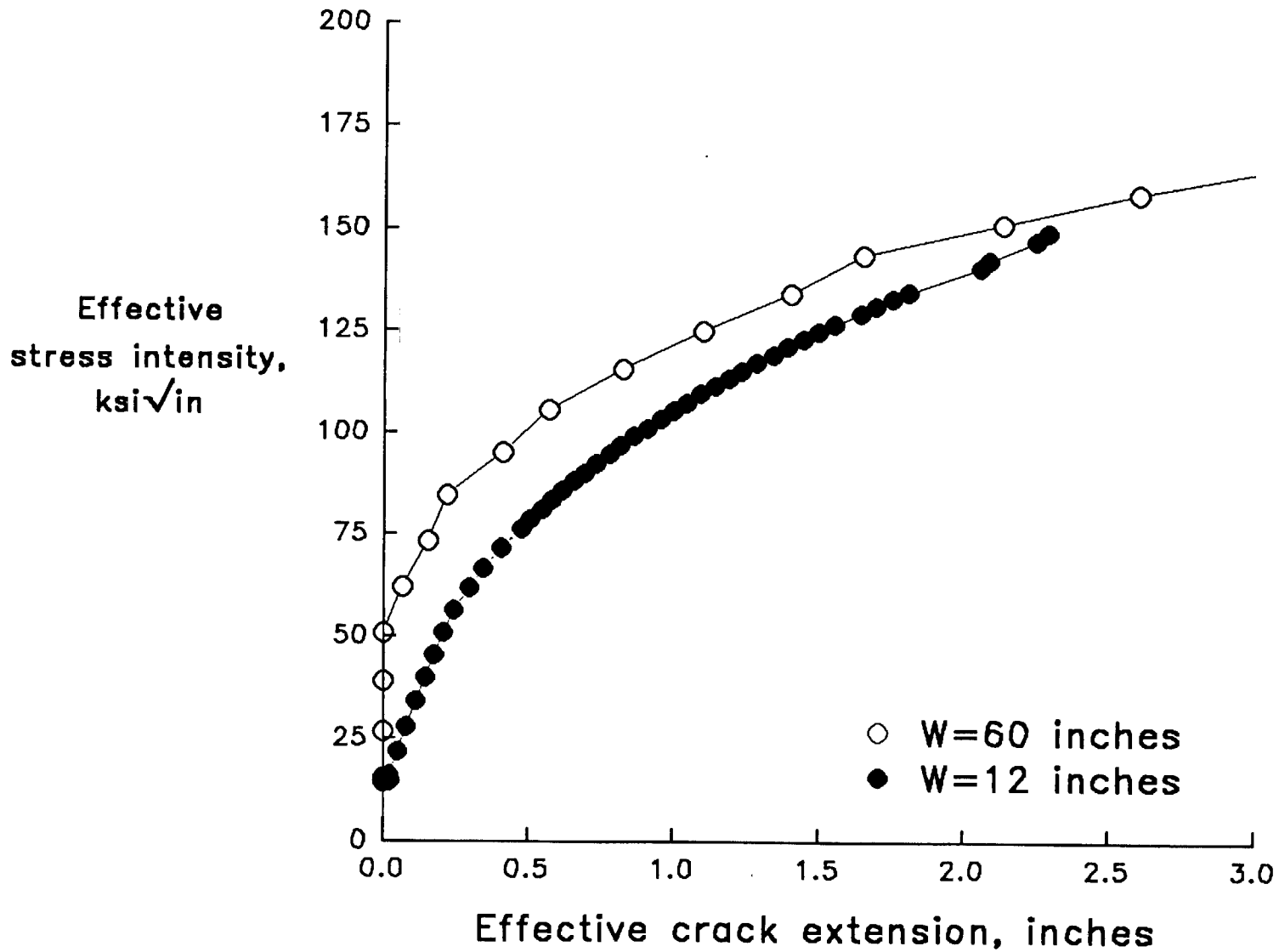


Figure 19. MT panel $K_{EFF}$–R curves, B=0.063 inches.

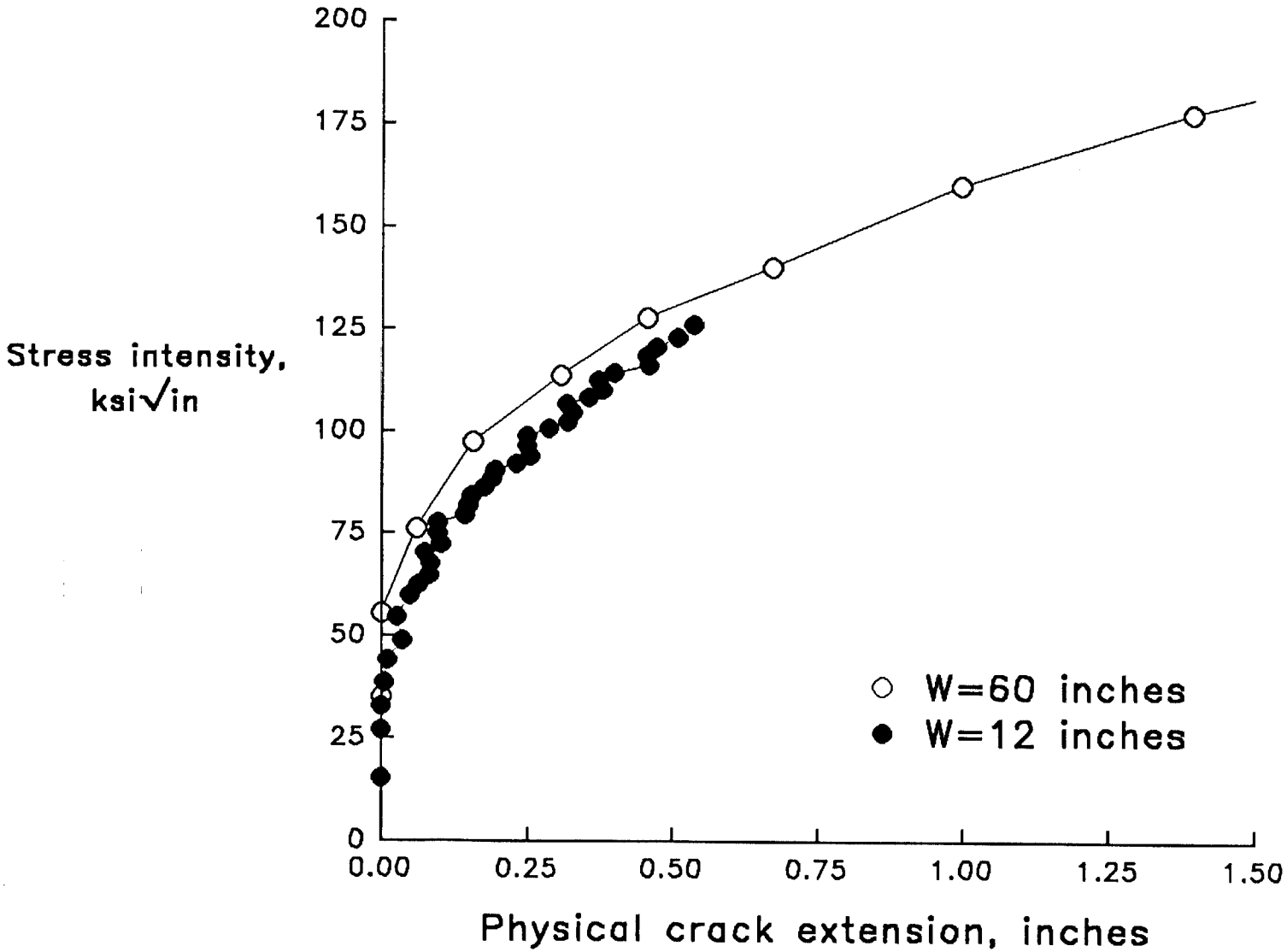


Figure 20. MT panel $K_J$–R curves, B=0.125 inches.

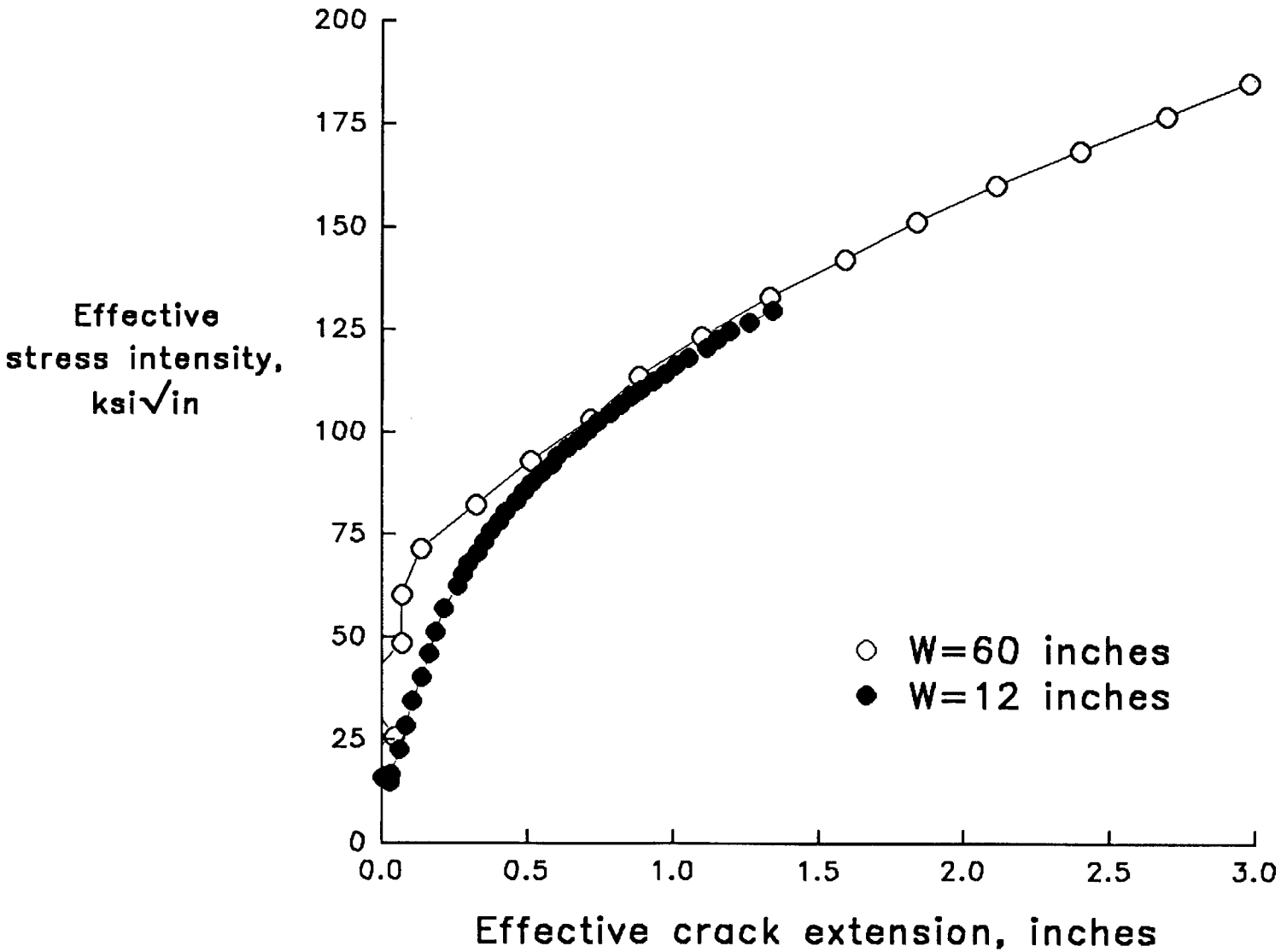


Figure 21. MT panel $K_{EFF}$–R curves, B=0.125 inches.

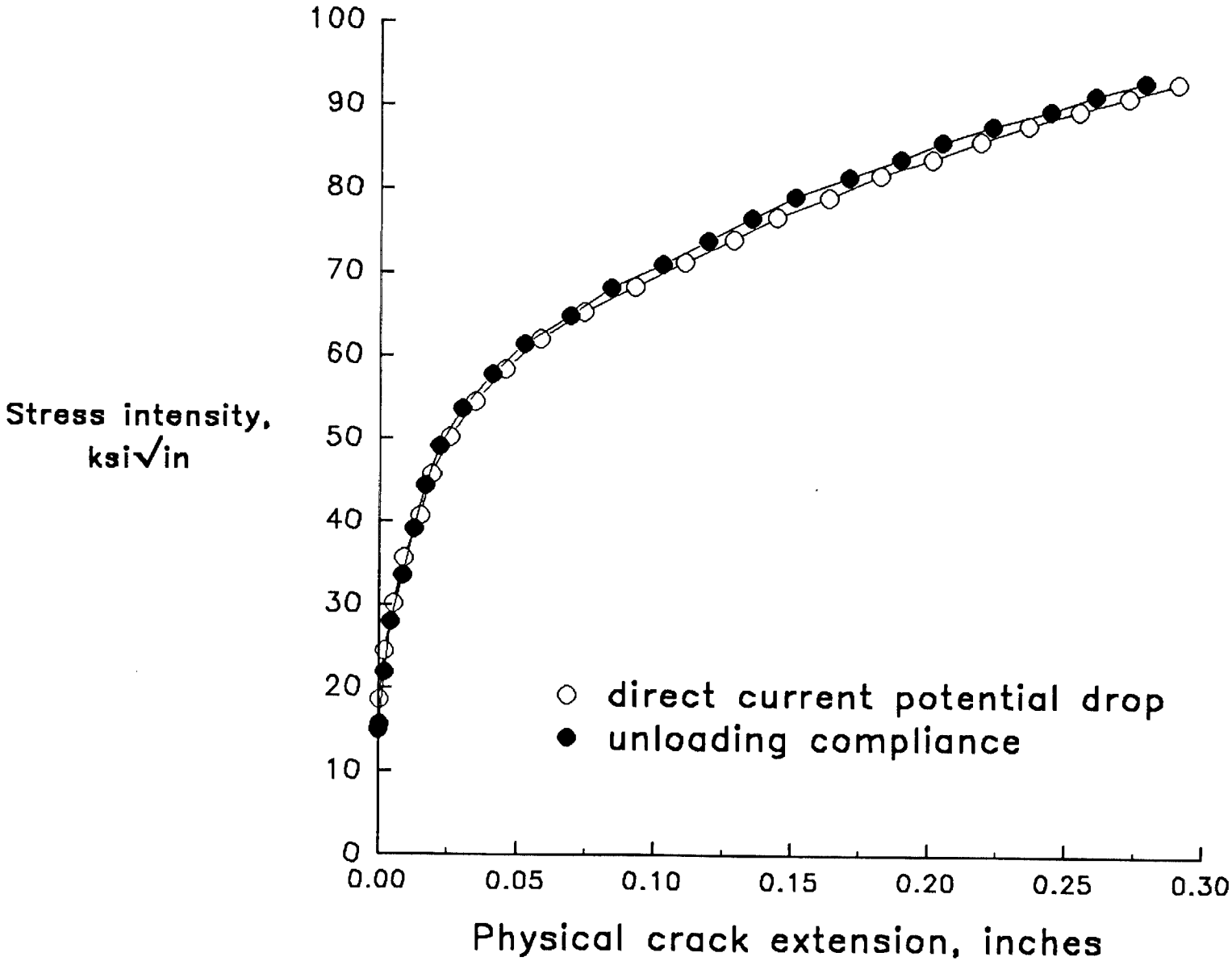


Figure 22. Comparison of crack length measurement methods for CT specimen $K_J$–R curves, W=2 inches, B=0.125 inches.

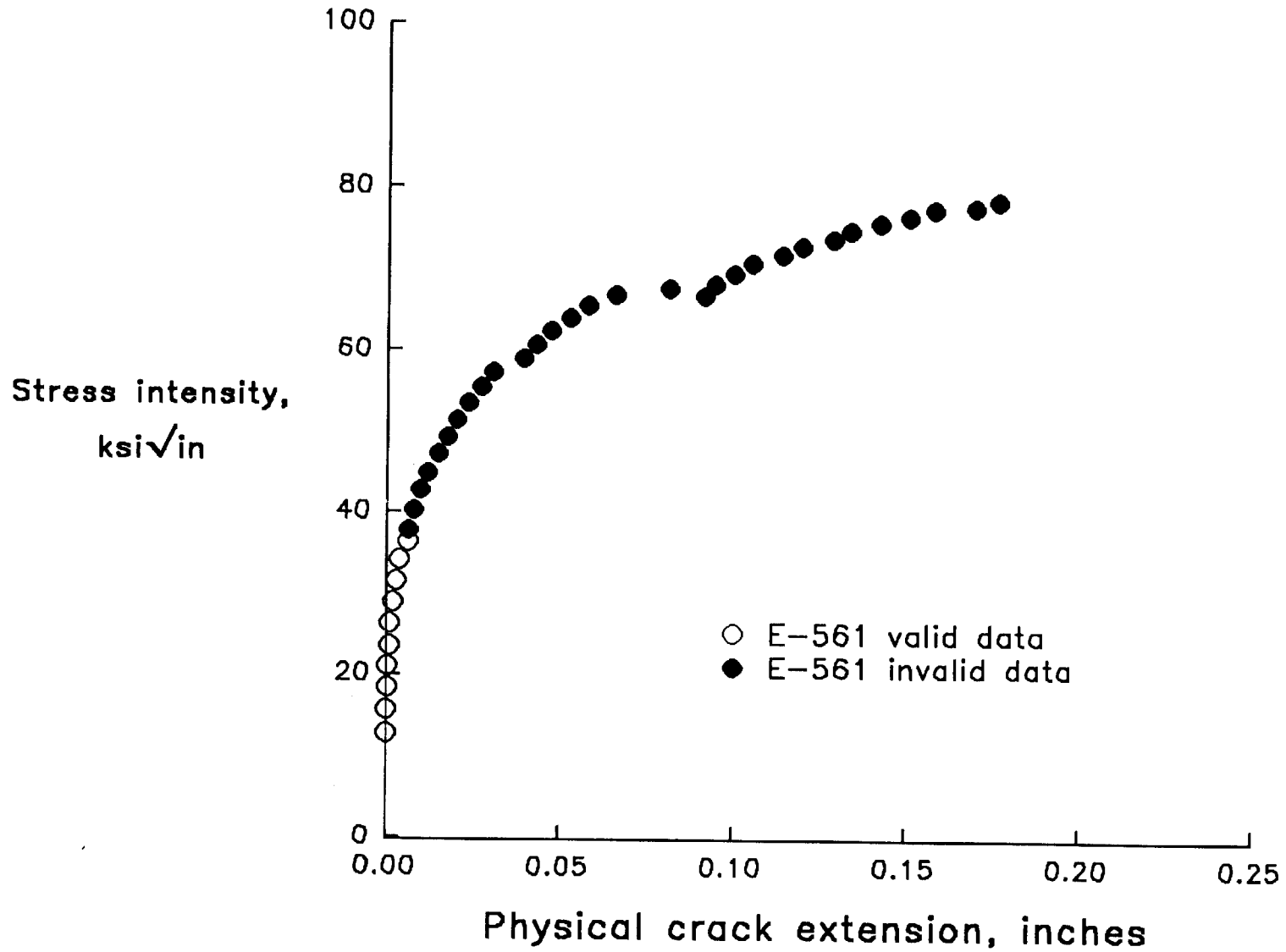


Figure 23. Valid and invalid CT specimen data, W=2 inches, B=0.125 inches.

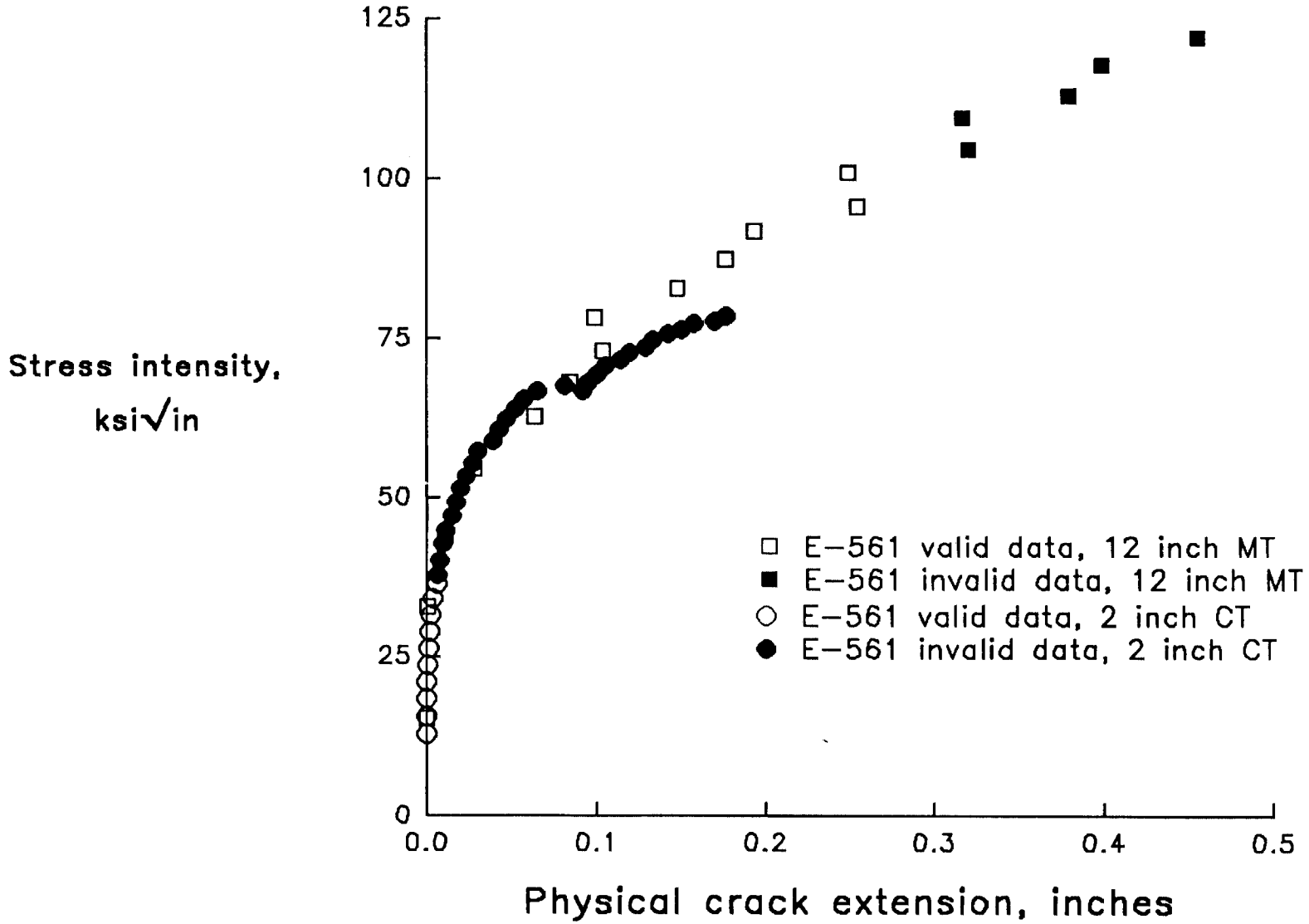


Figure 24. Comparison of valid and invalid data from CT and MT specimens, B=0.125 inches.

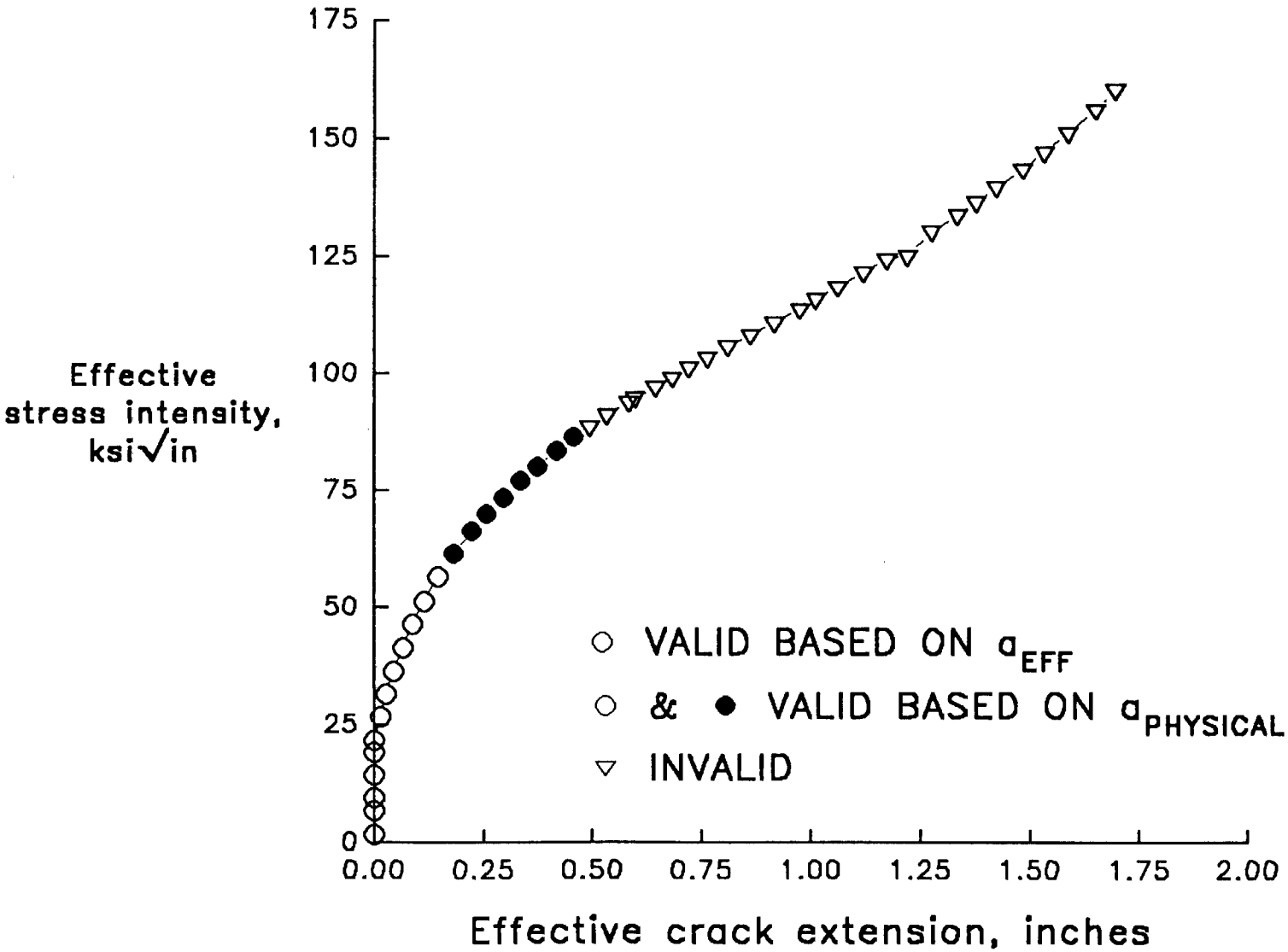


Figure 25. Validity based on net section stress < 0.8 yield stress for an MT specimen with W=6.3 inches and B=0.125 inches.

# REPORT DOCUMENTATION PAGE

*Form Approved*
*OMB No. 0704-0188*



| 1. AGENCY USE ONLY *(Leave blank)* | 2. REPORT DATE | 3. REPORT TYPE AND DATES COVERED |
|---|---|---|
| | October 1994 | Contractor Report |

**4. TITLE AND SUBTITLE**
Multi-Lab Comparison of R-Curve Methodologies: Alloy 2024-T3

**5. FUNDING NUMBERS**
C NAS1-19708
WU 537-06-20-06

**6. AUTHOR(S)**
Anthony P. Reynolds

**7. PERFORMING ORGANIZATION NAME(S) AND ADDRESS(ES)**
Analytical Services and Materials, Inc.
107 Research Drive
Hampton, VA 23666

**8. PERFORMING ORGANIZATION REPORT NUMBER**

**9. SPONSORING / MONITORING AGENCY NAME(S) AND ADDRESS(ES)**
National Aeronautics and Space Administration
Langley Research Center
Hampton, VA 23681-0001

**10. SPONSORING / MONITORING AGENCY REPORT NUMBER**
NASA CR-195004

**11. SUPPLEMENTARY NOTES**
Langley Technical Monitor: Ronald Clark
Final Report

**12a. DISTRIBUTION / AVAILABILITY STATEMENT**
Unclassified-Unlimited
Subject Category 26

**12b. DISTRIBUTION CODE**

**13. ABSTRACT** ***(Maximum 200 words)***

In an effort to determine an optimum method for ranking the fracture toughness of developmental aluminum alloys for High Speed Civil Transport applications, five labs performed K and/or J based fracture tests on aluminum alloy 2024-T3. Two material thicknesses were examined: 0.063 in. and 0.125 in. Middle crack tension and compact tension specimens were excised from 60 in. wide middle crack tension panels which had been previously tested at Boeing. The crack resistance curves generated were compared to the R-curves from 60 in. wide specimens. The experimental program indicated that effective stress intensity from secant compliance based crack length and stress intensity calculated from J-integral testing were equivalent. In addition, comparison of defferent specimen sezes and configurations indicated that standard validity requirements for compact tension specimens may be overly restrictive.

| 14. SUBJECT TERMS | 15. NUMBER OF PAGES |
|---|---|
| J-integral; Fracture toughness; Sheet material; R-curves; Aluminum alloys | 40 |
| | 16. PRICE CODE: A03 |

| 17. SECURITY CLASSIFICATION OF REPORT | 18. SECURITY CLASSIFICATION OF THIS PAGE | 19. SECURITY CLASSIFICATION OF ABSTRACT | 20. LIMITATION OF ABSTRACT |
|---|---|---|---|
| Unclassified | Unclassified | Unclassified | |